RKKY INTERACTION AND ITS CONTROL IN GRAPHENE AND RELATED MATERIALS

A Thesis Submitted to
the Graduate School of Engineering and Sciences of
İzmir Institute of Technology
in Partial Fulfillment of the Requirements for the Degree of
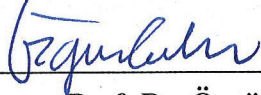
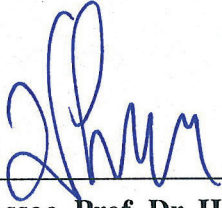**MASTER OF SCIENCE**

in Physics

by
Ahmet Utku CANBOLAT

July 2019
İZMİR

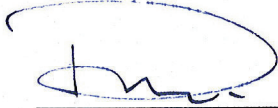We approve the thesis of **Ahmet Utku CANBOLAT**

Examining Committee Members:

_____
Assoc. Prof. Dr. Özgür ÇAKIR
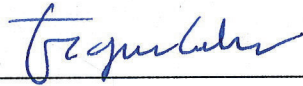Department of Physics, İzmir Institute of Technology

_____
Assoc. Prof. Dr. Hâldun SEVİNÇLİ
Department of Materials Science and Engineering, İzmir Institute of Technology

_____
Assoc. Prof. Dr. Cem SEVİK
Department of Mechanical Engineering, Eskişehir Technical University

12 July 2019

_____
Assoc. Prof. Dr. Özgür ÇAKIR
Department of Physics
İzmir Institute of Technology

_____
Prof. Dr. Lütfi ÖZYÜZER
Head of the Department of Physics

_____
Prof. Dr. Aysun SOFUOĞLU
Dean of the Graduate School of
Engineering and Sciences

ACKNOWLEDGEMENTS

ABSTRACT

RKKY INTERACTION AND ITS CONTROL IN GRAPHENE AND RELATED MATERIALS

Graphene got dramatic attention and lead the two-dimensional material physics after its first successful synthesis in 2004. Its unique electronic properties contain great potential for both scientific and technological applications. RKKY (Ruderman-Kittel-Kasuya-Yosida) is an indirect exchange interaction mediated by conduction electrons. In graphene, the interaction strength decay as $1/R^3$ where R is the distance between the magnetic moments. In the first part of this work, we calculated that applying circular potential on a graphene sheet forms quasi-bound states in the potential region. Via these states, the RKKY interaction is enhanced between magnetic moments on the edge of the potential well. This can be thought of an electronic analog of the Purcell effect. We showed that the interaction strength is even more enhanced if the Fermi level is in resonance with the energies of the quasi-bound states.

In the second part, we considered zigzag edged hexagonal nanoflakes. It is known that zigzag edged flakes have zero-energy edge-states. It is also known that the states with closer energies contribute more to RKKY interaction. Thus, we calculated that there is an enhancement between these edge-states.

In the third part, we investigated the behavior of RKKY interaction for two dimensional materials with quartic dispersion. An energy dispersion is said to be quartic if it is of the form $E = \alpha(k^2 - k_c^2)^2$. Here, α and k_c are material dependent constants. There are many materials exhibiting the quartic dispersion such as nitrogene, phosphorene, and arsenene. These materials are also sharing two-dimensional hexagonal lattice structure with graphene. What makes quartic dispersion special is that it has van-Hove singularity in its density of states near the band-edge. RKKY interaction is sensitive to the density of states because it depends on the number of electrons contributing spin exchange. Thus, the larger the number of electrons, the stronger the coupling. In this part, we tuned the Fermi level so that it lies on the DOS singularity and then we calculated the interaction strength as a function of R. We found a slowly decaying RKKY interaction for quartic dispersion. If the energy dispersion is pure quartic (i.e. $E = \alpha k^4$), we found the interaction strength depends on $1/(k_f R)$ instead of $1/R$ which makes the RKKY interaction long range for arbitrarily small Fermi level.

ÖZET

GRAFEN VE BENZERİ MALZEMELERDE RKKY ETKİLEŞİMİ VE KONTROLÜ

2004 yılında ilk kez başarıyla sentezlenmesinin ardından, grafene olan ilgi ciddi bir şekilde arttı ve grafen iki boyutlu malzeme fiziğinin başını çekti. Kendine özgü elektronik özellikleri hem bilimsel hem de teknolojik uygulamalar için büyük bir potansiyeldir. RKKY (Ruderman-Kittel-Kasuya-Yosida), iletim elektronları aracılığıyla gerçekleşen dolaylı değiş tokuş etkileşimidir. Etkileşim gücü grafende $1/R^3$ ile orantılıdır. Burada R manyetik momentler arası uzaklıktır. Bu çalışmanın ilk kısmında grafene uygulanan dairesel potansiyelin, potansiyel bölgesi içerisinde yarı-bağlı durumlar oluşturduğu ve bu durumlar üzerinden RKKY etkileşimin güçlendiği gösterilmiştir. Bu süreç Purcell etkisinin bir analojisi olarak düşünülebilir. Buna ek olarak, Fermi seviyesini potansiyel bölgesindeki yarı bağlı durumların enerjisi ile rezonans durumunda olmasının etkileşim gücünü daha da artırdığı gösterilmiştir.

İkinci kısımda, zigzag kenarlı altıgen nanopullar üzerinde RKKY etkileşimi incelenmiştir. Zigzag kenarlı nanopulların sıfır enerjili kenar durumları vardır ve yakın enerjili durumlar RKKY etkileşimine daha çok katkı sağlar. Bu nedenle RKKY etkileşimi bu kenar-durumları vasıtasıyla güçlenir.

Üçüncü kısımda ise RKKY etkileşimin kuartik enerji dağılımına sahip iki boyutlu malzemelerdeki davranışları incelenmiştir. Enerji dağılımı $E = \alpha(k^2 - k_c^2)^2$ formunda ise buna kuartik dağılım denir. Burada α ve k_c malzemeye özgü sabitlerdir. Bu enerji dağılımına uyan bir çok malzeme vardır. Bunlardan bazıları nitrojen, fosforen, arsenen'dir. Bu malzemeler de tıpkı grafen gibi altıgen örgü yapısında ve iki boyutludur. Kuartik dağılımı özel yapan, durum yoğunluğunun bant sınırındaki van-Hove tekilliğidir. RKKY etkileşimi durum yoğunluğuna hassas bir şekilde bağlıdır. Bunun nedeni etkileşime çoğunlukla Fermi seviyesi civarındaki elektronların katkıda bulunmasıdır. Eğer Fermi seviyesi etrafında çok sayıda elektron varsa, etkileşim gücü de buna bağlı olarak artar. Bu bölümde Fermi seviyesini durum yoğunluğunun tekilliğine denk gelecek şekilde ayarlandı ve etkileşim gücünü R'ye bağlı olarak hesaplandı. Sonuçta RKKY etkileşiminin yavaş sönümlendiğini bulundu. Enerji dağılımının saf kuartik olduğu durumda (diğer bir deyişle $E = \alpha k^4$), etkileşim gücünün $1/R$ ile değil $1/(k_f R)$ ile orantılı olduğu bulundu. Bu da bant sınırına yakın Fermi seviyeleri için RKKY etkileşiminin uzun erimli olduğunu gösterir.

TABLE OF CONTENTS

LIST OF FIGURES

LIST OF TABLES

CHAPTER 1

INTRODUCTION

Carbon is an essential element so that it is the root of many molecules from the simplest ones to complex ones such as amino acids and proteins. This is because it is highly abundant and the flexibility of carbon atoms due to their four valence electrons allow them to form complex structures. Carbon has different allotropes like diamond, graphite and graphene. Diamond and graphite are very well-known materials. Although graphene is known for many years, it is first synthesized successfully in 2004 by a clever method Novoselov et al. (2004). Graphene is a single layer material. It has a hexagonal lattice structure (also commonly called honeycomb lattice because of the visual similarities) and only carbon atoms are attached the lattice sites. Even if graphene is single layer, it is extraordinally strong mechanically. It has very high thermal and electrical conductivity. With all these properties, it contains great applications in both science and technology (Novoselov et al., 2012; Geim and Novoselov, 2007; Choi et al., 2010; Castro Neto et al., 2009).

One of the greatest properties of graphene is its linear energy dispersion at the edge of Brillouin zone. This relativistic behavior allows to be observed high-energy physics phenomenon such as atomic collapse (Wang et al., 2013; Shytov et al., 2007) and Klein tunneling (Katsnelson et al. (2006b)) in a solid state system. The linear dispersion is also responsible for highly mobile electrons in graphene.

RKKY interaction is an indirect exchange interaction mediated by conduction electrons. It is known for many years and independently found by four physicists Ruderman, Kittel, Kasuya and Yosida (Ruderman and Kittel, 1954; Kasuya, 1956; Yosida, 1957). In this work, RKKY interaction is investigated in various systems. The work consists of three parts. Each parts emphasis on closely related but different problems. The motivation is to find enhanced RKKY interaction by manipulating electronic and geometric properties of graphene and related two dimensional materials.

In the first part, we considered a graphene sheet under applied circular potential. It is experimentally shown that applying circular potential on graphene forms whispering-gallery modes in the potential region (Zhao et al., 2015). RKKY interaction is extensively studied for pristine graphene (Kogan, 2011; Black-Schaffer, 2010b; Sherafati and Satpathy, 2011; Saremi, 2007). All the researches agree on RKKY interaction decay as $1/R^3$

where R is the distance between the magnetic moments. We calculated that the interaction enhanced via these bound states confined in the potential region.

In the second part, we calculated RKKY interaction for zigzag edged hexagonal graphene nanoflakes. There are many structure can be made out of graphene by changing its geometry such as carbon nanotubes, nanoribbons, nanoflakes and nanowires. The zigzag edged hexagonal graphene flakes are special because they have edge-states with zero energy (Fujita et al., 1996; Nakada et al., 1996; Zarenia et al., 2011). We know that RKKY interaction is sensitive to states with close energies. Thus, we expect a long range RKKY behavior between these edge states.

In the third part, we did not consider graphene but consider other closely related two dimensional materials such as phosphorene, arsenene and bizmuthene. These materials are two dimensional and, like graphene, they have hexagonal lattice. What make these materials special is that they have quartic energy dispersion (Sevinçli, 2017). A dispersion is said to be quartic if it is of the form $E = \alpha(k^2 - k_c^2)^2$ where α and k_c are material dependent constants. If $k_c = 0$, then the energy dispersion is called pure quartic. Materials with quartic and pure quartic dispersion have strong van-Hove singularities in their density of states. We calculated that RKKY interaction is enhanced if we tune Fermi level on these singularities. It is because there are many states that can contribute to the interaction.

1.1. Graphene

Graphene has hexagonal lattice structure as can be seen in the figure 1.1 .All atomic sites are not equivalent. Thus, graphene is not a Bravais lattice. We think of a graphene as a two interpenetrating triangular sublattices. These sublattices are called A and B. It does not matter which sublattice is called A or B due to the symmetry. Carbon has four valence electrons and three of them make sp^2 bonding with their nearest neighbors. One electron remains unpaired in the p$_z$ orbital and it freely moves in graphene. The lattice vectors are

$$a_1 = \frac{a}{2}(3, \sqrt{3}) \qquad\qquad a_2 = \frac{a}{2}(3, -\sqrt{3}) \qquad\qquad (1.1)$$

Here, a is the interatomic distance and it is approximately 1.42 Å. As can be seen in figure 1.1, δ vectors are the nearest neighbor vectors and it is often useful to work with

those vectors. The Brillouin zone and the reciprocal lattice vectors can be seen in figure 1.2. The reciprocal lattice vectors are

$$b_1 = \frac{2\pi}{3a}(1, \sqrt{3}) \qquad\qquad b_2 = \frac{2\pi}{3a}(1, -\sqrt{3}) \qquad (1.2)$$

K and K' have a great importance which be covered in detail in section 1.1.2. K and K' points are called Dirac points and their positions in the reciprocal lattice are

$$K = \left(\frac{2\pi}{3a}, \frac{2\pi}{3\sqrt{3}a} \right) \qquad\qquad K' = \left(\frac{2\pi}{3a}, -\frac{2\pi}{3\sqrt{3}a} \right) \qquad (1.3)$$

There are three K and K' Dirac points in the Brilloin zone and the positions of these special points in the Brioullin zone can be seen in figure 1.2.
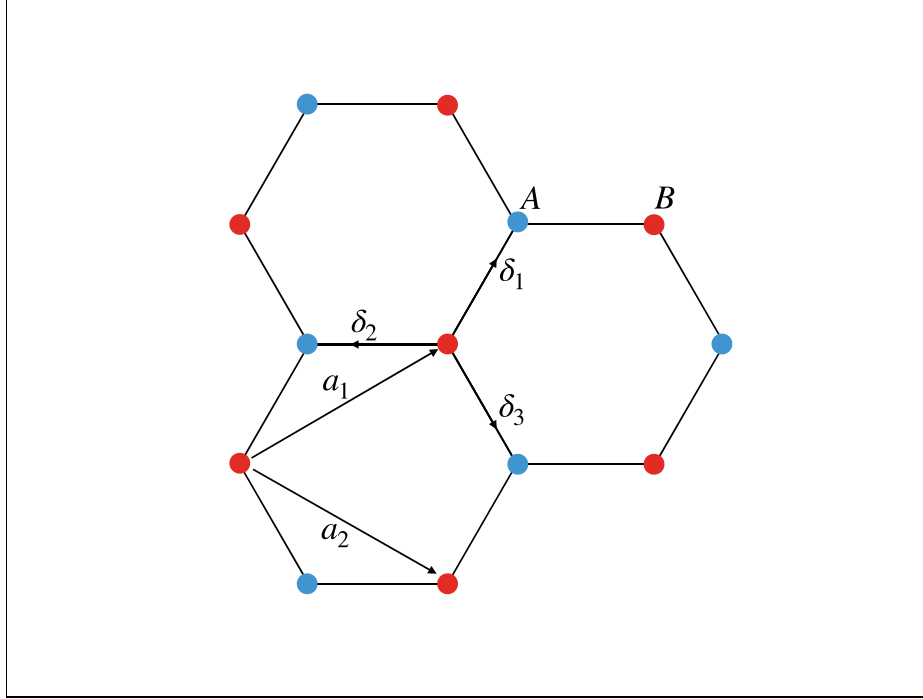
Figure 1.1. Hexagonal lattice structure of graphene. Blue and red points show the corresponding sublattices. a_1 and a_2 are the lattice vectors and, δ's are the nearest neighbor vectors.

There are two different directions in a hexagonal lattice. These are zigzag and armchair directions as shown in figure 1.3. These direction are often essential when considering especially nanoflakes. They determines the electronic properties of nanoflakes. The choose of the directions also determines the behavior of RKKY interaction in graphene which is covered in detail in RKKY section.
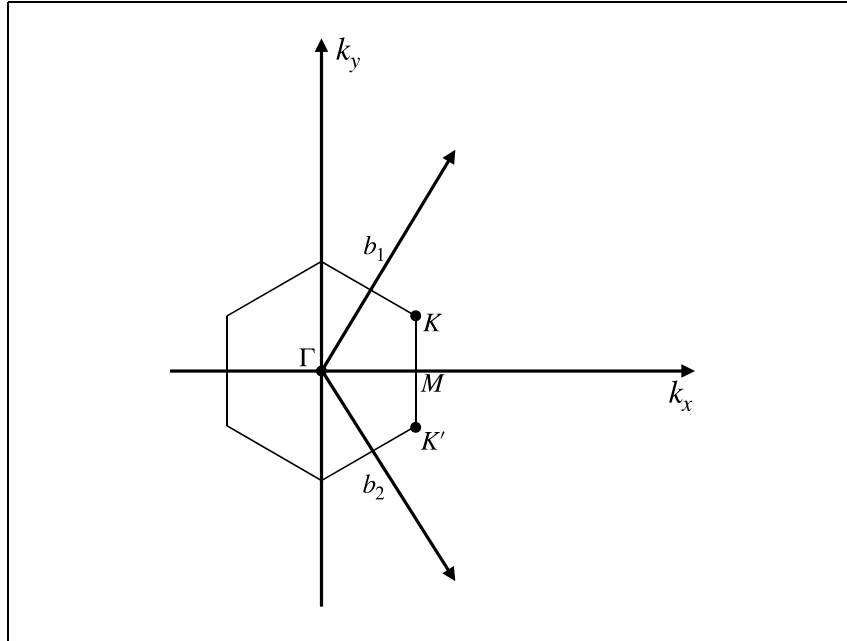
Figure 1.2. The Brillouin zone and the reciprocal lattice vectors b_1 and b_2. Γ is the zone center and K and K' points are the Dirac points.

1.1.1.   Tight Binding Approximation

Many methods have been developed to calculate the electronic properties of materials (Marder, 2010; Kittel, 2004). They can be organized under two categories. One is the free electron model/approximation. In this model, electrons are assumed to move freely in the material like gas molecules in an empty box. The wavefunctions are the same as the solution of the infinite square-well problem. The material plays no role but confining the electrons. It affects only the normalization of the wavefunction. This model can be modified to nearly-free electron model by introducing the crystal potential. In this case, electrons do not freely move but feel weak periodic potential due to absence of atoms in the crystal. This is, of course, more realistic than the free electron model.

The other limiting case is where electrons are localized on lattice sites. They do not move freely but they hop one lattice site to another instead. This model is called tight-binding model (or approximation) since the electrons are tightly bounded to lattice sites. It is convenient to start with introducing Wannier functions. Since we are dealing with the localized states, it is natural to consider atomic wave functions. Wannier functions are the orthogonal set of states and they obey the Bloch's theorem due to the translational symmetry of lattice. Thus, Wannier functions can be written as Bloch functions. For a
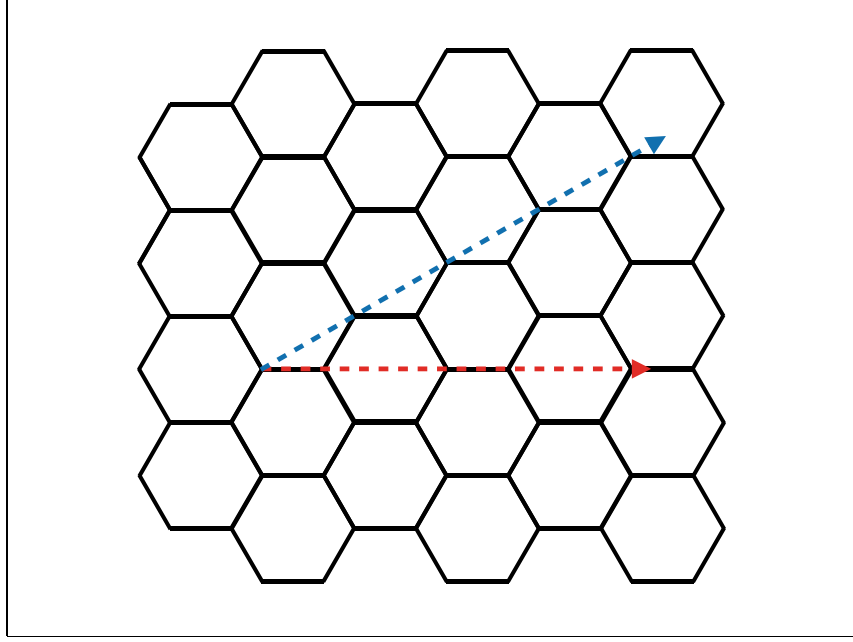
Figure 1.3. Blue dashed line shows the zigzag direction and red dashed line shows the
armchair direction.

lattice site R, the Wannier function is defined as

$$\langle r|R\rangle \equiv w_n(R,r) = \frac{1}{\sqrt{N}} \sum_k e^{-ik\cdot R} \psi_{nk}(r) \tag{1.4}$$

Here, N is the number of sites, r is the position in three dimension, n is the band
index, and R is the coordinate of the lattice site we are interested in. Using the definition,
one can show the orthogonality of the Wannier functions.

$$\int dr\, w_n(R,r) w_m^*(R',r) = \int dr \sum_{k,k'} \frac{1}{N} e^{-ik\cdot R + R'\cdot k'} \psi_{nk}^*(r) \psi_{mk'}(r) \tag{1.5}$$

$$= \frac{1}{N} \sum_{k,k'} \frac{1}{N} e^{-ik\cdot R + R'\cdot k'} \delta_{mn}\delta_{kk'} = \delta_{mn}\delta_{RR'}$$

Wannier functions are localized at R but they do not rapidly decay with R. They
also form a complete orthogonal set of states. Thus, we can write Schrodinger equation
in Wannier function basis.

$$H = \sum_{RR'} |R'\rangle \langle R'| H |R\rangle \langle R| \tag{1.6}$$

5

Here we denoted $w_n(R, r)$ by $|R\rangle$. Notice that the Hamiltonian only describes the nth band because one can easily show that the overlaps of Wannier functions between different bands vanish. Let us write down the matrix elements explicitly.

$$H_{RR'} = \langle R' | H | R \rangle = \int dr \, w_n^*(R', r) \left(-\frac{\hbar^2 \nabla^2}{2m} + U(r) \right) w_n(R, r) \qquad (1.7)$$

This is where we introduced the tight binding approximation. We are neglecting all the matrix elements unless R and R' are the nearest neighbors. This assumption allows only the hopping among nearest sites. Hence, only important thing that determines the matrix elements is the distance between lattice sites $R - R'$. Due to the symmetry the matrix elements involving R and R' can be considered with one parameter t. t is said to be hopping parameter or hopping amplitude which describes the transition probability from one site to other nearest sites. If system consists of different type of atoms, then the hopping parameter between different atoms becomes of course different. In this case, the summation will be slightly modified and it will contain different hopping parameter for different nearest neighbors. However, the structure of the Hamiltonian remains the same. The matrix elements $\langle R | H | R \rangle$ are constant and denoted by U. It is called on-site term and it describes the required energy to put one electron at a lattice site. It gives a system nothing but constant energy shift. The tight binding Hamiltonian can be finally written in the following form.

$$H_{TB} = \sum_{R\delta} |R\rangle \, t \, \langle R + \delta| + \sum_R |R\rangle \, U \, \langle R| \qquad (1.8)$$

where δ's are nearest neighbor lattice vectors pointing from R. In literature, the occupation number representation is more widely used for H_{TB} which can be easily written in this form as follows:

$$H_{TB} = t \sum_{<i,j>} c_i^\dagger c_j \qquad (1.9)$$

where $c_i^\dagger$ and c_j are the creation and annihilation operators, respectively. What this Hamiltonian describes is to destroy one electron from site j and put it at the site i with the hopping amplitude of t. The term under the summation $< i, j >$ means that we are only taking nearest sites into account. If the term were $<< i, j >>$, then this would mean that we are also considering second nearest sites. Then, the Hamiltonian takes the form

$$H_{TB} = t_1 \sum_{<i,j>} c_i^\dagger c_j + t_2 \sum_{<<i,j>>} c_i^\dagger c_j \qquad (1.10)$$

Here, it should be noticed that we now have two hopping parameters t_1 and t_2. $t_1 > t_2$ because it is harder to hop further sites since the wave functions less likely overlap.

1.1.2. Tight Binding Description of Graphene

Tight binding description first introduced by Wallace in 1946 (Wallace, 1947; Bena and Montambaux, 2009; Guclu et al., 2014; Saito et al., 1998; Reich et al., 2002).Valance electrons of carbon atoms make sp^2 hybridization with the nearest carbon atoms and one electron remains unpaired as mentioned in the introduction. We can describe the nature of this unpaired electrons using tight binding method. Graphene has a honeycomb lattice which is not a Bravais lattice. Thus, we should think of the lattice as two interpenetrating triangular sublattices. Let us name one sublattice A and the other one B. Then, the following vectors span all real points in the lattice:

$$R_A = na_1 + ma_2 + b \qquad (1.11)$$

$$R_B = na_1 + ma_2 \qquad (1.12)$$

Here, a_1 and a_2 are the primitive lattice vectors. n and m are integers. b is the vector between A type and B type atom in a unit cell. We can now use Bloch's theorem since we have translation symmetry in the system. The wavefunction of an electron at R_A can be written as a linear combination of p_z orbitals of same sublattice.

$$\Psi_k^A(r) = \frac{1}{\sqrt{N}} \sum_{R_A} e^{ikR_A} \phi_z(r - R_A) \qquad (1.13)$$

$$\Psi_k^B(r) = \frac{1}{\sqrt{N}} \sum_{R_B} e^{ikR_B} \phi_z(r - R_B) \qquad (1.14)$$

Here, N is the number of unit cells. We are assuming that the p_z orbitals form complete orthogonal set of states because we, in the beginning, assumed that p_z orbitals are very localized so that they do not have overlapping wavefunctions. The total wavefunction is the linear combination of the wave functions Ψ_A and Ψ_B:

$$\Psi_k(r) = \alpha \Psi_k^A(r) + \beta \Psi_k^B(r) \tag{1.15}$$

All we should do is to determine α and β by diagonalizing the Hamiltonian.

$$H = \frac{p^2}{2m} + \sum_{R_A} V(r - R_A) + \sum_{R_B} V(r - R_B) \tag{1.16}$$

where $V(r - R)$ is the atomic potentials at R. Then the Hamiltonian can be written in matrix form as

$$H(k) = \begin{pmatrix} \left\langle \Psi_k^A \middle| H \middle| \Psi_k^A \right\rangle & \left\langle \Psi_k^A \middle| H \middle| \Psi_k^B \right\rangle \\ \left\langle \Psi_k^B \middle| H \middle| \Psi_k^A \right\rangle & \left\langle \Psi_k^B \middle| H \middle| \Psi_k^B \right\rangle \end{pmatrix} \tag{1.17}$$

We could solve the Hamiltonian exactly but it will be easier if we make few assumptions. First, we can assume that $\epsilon_A(k) = 0$ because we only consider the nearest neighbor hopping. Second, we can neglect the onsite energies which are the terms $\left\langle \Psi_k^A \middle| H \middle| \Psi_k^A \right\rangle$ and $\left\langle \Psi_k^B \middle| H \middle| \Psi_k^B \right\rangle$ in the Hamiltonian. Only the off-diagonal terms survived. If we write them explicitly, we obtain

$$\left\langle \Psi_k^B \middle| H \middle| \Psi_k^A \right\rangle = \frac{1}{N} \sum_{<R_A, R_B>} e^{ik(R_A - R_B)} \int dr \phi_z^*(r - R_B) V(r - R_B) \phi_z(r - R_A) \tag{1.18}$$

When we closely look at the integral, we can see that it is constant regardless of the choice of R_A and R_B as long as they are nearest neighbors. Thus, we can define a hopping parameter:

$$t \equiv \int dr \phi_z^*(r - R_B) V(r - R_B) \phi_z(r - R_A) \tag{1.19}$$

One can either calculate t using the orbital states $\phi_z(r - R)$. However, it is easier to use the experimental results for the nearest neighbor hopping parameter t which is approximately -2.8 eV. All is left to substitute nearest neighbor vectors R_A and R_B to get final form of the Hamiltonian.

$$\left\langle \Psi_k^A \middle| H \middle| \Psi_k^B \right\rangle = t \sum_{<R_A, R_B>} e^{ik(R_A - R_B)} = t \left(e^{-ikb} + e^{-ik(b-a_1)} + e^{-ik(b-a_2)} \right) \tag{1.20}$$

and also the other of diagonal term should of course be the Hermitian conjugate of the expression above.

$$\left\langle \Psi_k^B \right| H \left| \Psi_k^A \right\rangle = t \sum_{<R_A, R_B>} e^{ik(R_A - R_B)} = t \left(e^{ikb} + e^{ik(b-a_1)} + e^{ik(b-a_2)} \right) \qquad (1.21)$$

In literature, it is common to define a function $f(k)$ to have more compact form. Define $f(k)$ as follows

$$f(k) \equiv e^{-ikb} + e^{-ik(b-a_1)} + e^{-i(b-a_2)} \qquad (1.22)$$

Hence, we finally obtain the tight binding Hamiltonian for graphene as

$$H(k) = t \begin{pmatrix} 0 & f(k) \\ f^*(k) & 0 \end{pmatrix} \qquad (1.23)$$

Now, we should find the eigenvalues and eigenfunctions of the Hamiltonian by solving the eigenvalue equation below

$$E(k) \begin{pmatrix} \alpha \\ \beta \end{pmatrix} = t \begin{pmatrix} 0 & f(k) \\ f^*(k) & 0 \end{pmatrix} \begin{pmatrix} \alpha \\ \beta \end{pmatrix} \qquad (1.24)$$

The eigenvalues of the Hamiltonian are

$$E_{\pm}(k) = \pm |tf(k)| \qquad (1.25)$$

The positive energy solution corresponds to conduction band and the negative energy solution corresponds to valence band. The corresponding eigenfunctions are

$$\Psi_k^+(r) = \frac{1}{\sqrt{2N}} \left(\sum_{R_A} e^{ikR_A} \phi_z(r - R_A) - \sum_{R_B} e^{ikR_B} \frac{f^*(k)}{|f(k)|} \phi_z(r - R_B) \right) \qquad (1.26)$$

$$\Psi_k^-(r) = \frac{1}{\sqrt{2N}} \left(\sum_{R_A} e^{ikR_A} \phi_z(r - R_A) + \sum_{R_B} e^{ikR_B} \frac{f^*(k)}{|f(k)|} \phi_z(r - R_B) \right) \qquad (1.27)$$

As can be seen on the plot of the energy dispersion, graphene does not have a bandgap. In Brillouin zone, there are six points named K and K' where the conduction and valence band touch. These points are called Dirac points. Since graphene does not have a bandgap but the valence and conduction band touch only some points, it is considered as a semimetal. The Fermi level lies on these Dirac points and the system has a
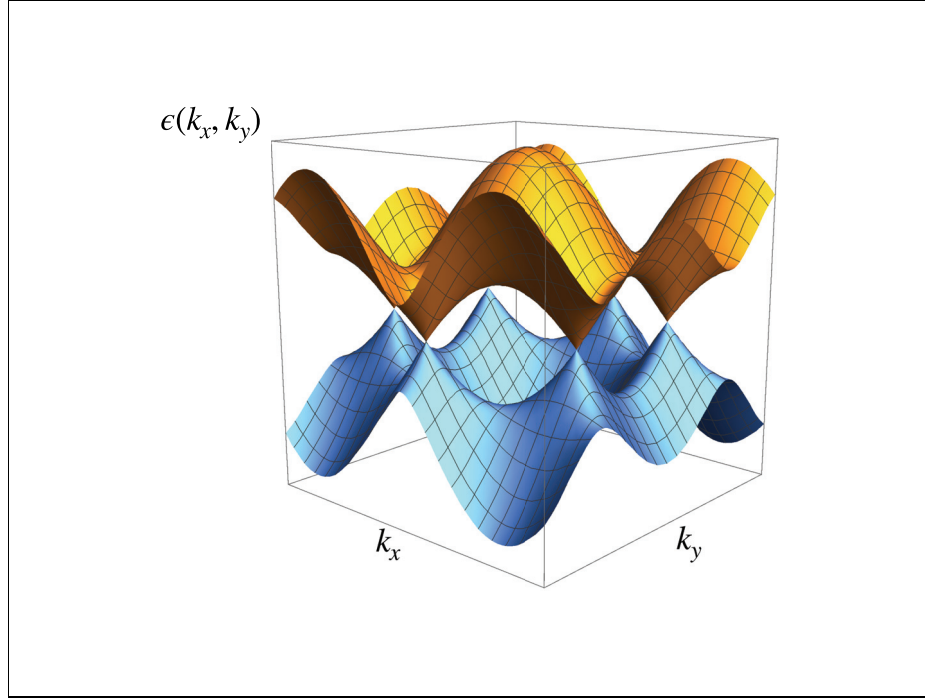
Figure 1.4. The energy bands of graphene. The orange part is the conduction band and the blue part is the valence band. The points where the conduction and valence band touch are the Dirac points.

circular symmetry around these points. Because the electronic properties are determined by the electrons near Fermi level, it is convenient to expand $E(k)$ around K and K' points. This expansion is enough to describe low-energy electrons.

We know that $E_\pm = \pm|tf(k)|$ and $K = (4\pi/(3\sqrt{3}a), 0)$. Then,

$$f(K + q) = f(K) + f'(K)q + ... \tag{1.28}$$

where q is the vector in k-space which measured from K. Keeping only first order terms yield

$$f(K + q) \approx -\frac{3}{2}a(q_x - \mathrm{i}q_y) \tag{1.29}$$

Let $E_K(q)$ and be the energy eigenvalue around K point as a function of q. Then, the effective Schrödinger equation can be written as

$$E_K(q) \begin{pmatrix} \alpha_q \\ \beta_q \end{pmatrix} = -\frac{3}{2}ta \begin{pmatrix} 0 & q_x - \mathrm{i}q_y \\ q_x + \mathrm{i}q_y & 0 \end{pmatrix} \begin{pmatrix} \alpha_q \\ \beta_q \end{pmatrix} \tag{1.30}$$
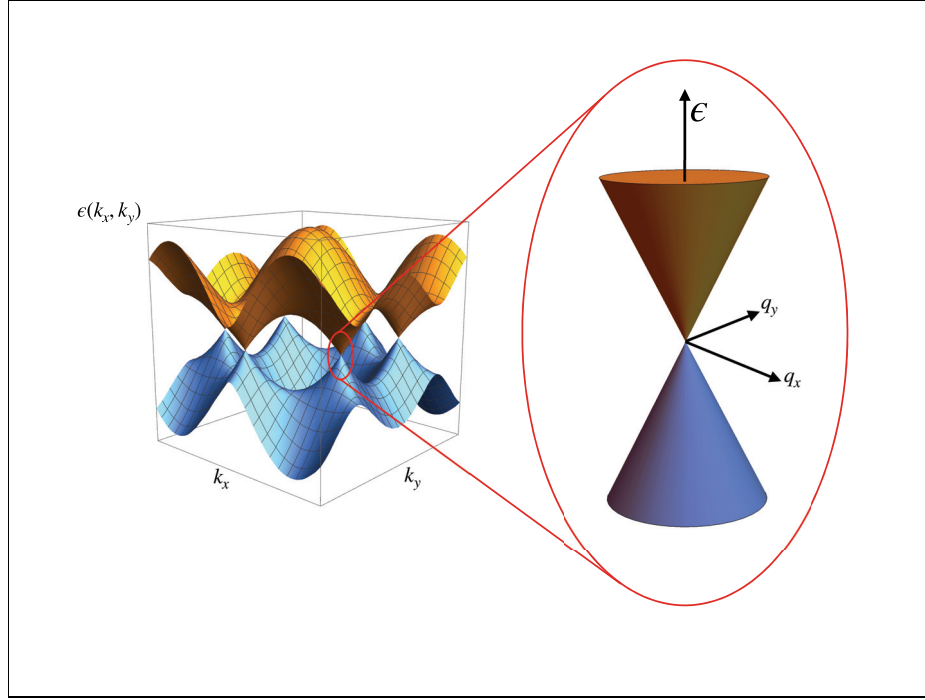
Figure 1.5. The linear behaviour of the energy dispersion near a Dirac point.

Solving the eigenvalue equation gives the eigenstates and eigenvalues.

$$\psi_K^c(q) = \frac{3}{2}a|t||q| \tag{1.31}$$

$$\psi_K^v(q) = -\frac{3}{2}a|t||q|$$

Here, $\psi_K^c(q)$, $\psi_K^v(q)$ are the energies of electrons moving conduction and valence band, respectively. The correspoding eigenstates are

$$\psi_K^c(q) = \frac{1}{\sqrt{2}}\begin{pmatrix} 1 \\ e^{i\phi} \end{pmatrix} \tag{1.32}$$

$$\psi_K^v(q) = \frac{1}{\sqrt{2}}\begin{pmatrix} 1 \\ -e^{i\phi} \end{pmatrix}$$

where ϕ is the angle between q_x and q_y and it can be found by $\phi = \arctan(q_y/q_x)$. In literature, It is also a convention to write the eigenstate as

$$\psi_K(q) = \frac{1}{\sqrt{2}}\begin{pmatrix} 1 \\ \alpha e^{i\phi} \end{pmatrix} \tag{1.33}$$

11

Here, α is called band index and takes values of $+1$ for conduction and -1 for valence band. The upper part and lower part of the eigenstate describe the electrons moving in different sublattices. It is logical that there is only a phase factor otherwise the symmetry would be broken. Due to the spin-like property of the eigenstates/wavefunction, it is called pseudo-spinor.

Define the Fermi velocity $v_F = 3ta/2$. Then, The effective Hamiltonian then becomes

$$H_K = -iv_f\sigma \cdot \nabla \tag{1.34}$$

where σ is the Pauli matrix. The effective Hamiltonian plays a critical role because it is actually the massless Dirac equation which describes the motion of relativistic particles. It allows us to observe phenomena related to special relativity such as Klein tunneling, which is covered in detail in the next section. Here, the Fermi velocity $v_F \approx 10^6 m/s$ and it is 300 times slower than the speed of light. The electrons can be thought as the analogue of light in graphene.

1.2. Dirac Equation and Klein Tunneling

Graphene has many unique properties. One of them is its linear energy dispersion at K and K' points. As described in the previous chapter in detail, the tight-binding Hamiltonian takes the form of massless Dirac equation. The Dirac equation describes the behavior of relativistic particles. Graphene is very special in that manner because one can test high-energy physics phenomena such as atomic collapse or Klein tunneling in a solid state system. After P.A.M. Dirac established the Hamiltonian, Oscar Klein solved the equation for tunneling problems in 1929 (Greiner et al., 1985; Katsnelson et al., 2006a; Allain and Fuchs, 2011; Young and Kim, 2009). There cannot be a paradox in nature of course but the result was extremely counter-intuitive and that is why the phenomenon is often called Klein Paradox. As will be described in detail in this chapter, particles which come to a potential barrier passes through the barrier regardless of their energies. For non-relativistic particles, it expected to see an exponential decay in their wavefunctions. This unusual behavior is extremely important because it seriously affects confinements in graphene. For the calculation of RKKY interaction under applied circular potential, it is essential to consider what type of potential we choose. In this chapter, we will derive Dirac equation and investigate the behavior of the solutions for potential barrier problems.

Schrodinger equation does not describe relativistic particles (Greiner and Bromley, 2000). For a relativistic particle, Hamiltonian is

$$H = \sqrt{c^2 p^2 + m^2 c^4} \tag{1.35}$$

here, c, p and m are the speed of light, the momentum of the particle and the mass of the particle, respectively. The problem with this expression is that p is an operator and square root of an operator is undefined. There are two approaches to solve this problem. One is to expand the square-rooted term in series. This leads us to Klein-Gordon equation. The other method was proposed by P.A.M. Dirac. He claims that we can get rid of the square root by writing the term inside as whole square. Mathematically,

$$c^2 p^2 + m^2 c^4 = \left(c\alpha_x p_x + c\alpha_y p_y + c\alpha_z p_z + \beta m c^2 \right)^2 \tag{1.36}$$

All we need is to determine the matrices $\alpha_x, \alpha_y, \alpha_z$ and β which satisfy the equation above. If we expand expression, we get

$$
\begin{aligned}
c^2 p^2 + m^2 c^4 = \quad & (c^2 \alpha_x^2 p_x^2 + c^2 \alpha_y^2 p_y^2 + c^2 \alpha_z^2 p_z^2 + \beta^2 m^2 c^4) \\
& + c p_x p_y (\alpha_x \alpha_y + \alpha_y \alpha_x) + c p_y p_z (\alpha_y \alpha_z + \alpha_z \alpha_y) \\
& + c p_x p_z (\alpha_x \alpha_z + \alpha_z \alpha_x) + m c^3 p_x (\alpha_x \beta + \beta \alpha_x) \\
& + \text{other cross terms}
\end{aligned} \tag{1.37}
$$

The following conditions are needed to satisfy the equation above:

$$\alpha_i^2 = 1, \quad \beta^2 = 1, \quad \{\alpha_i, \alpha_j\} = 0, \quad \{\alpha_i, \beta\} = 0 \tag{1.38}$$

where i, j are the coordinate indices x, y, z and $i \neq j$. The following matrices meet these requirements:

$$\alpha_x = \begin{pmatrix} 0 & 0 & 0 & 1 \\ 0 & 0 & 1 & 0 \\ 0 & 1 & 0 & 0 \\ 1 & 0 & 0 & 0 \end{pmatrix} \qquad \alpha_y = \begin{pmatrix} 0 & 0 & 0 & i \\ 0 & 0 & -i & 0 \\ 0 & i & 0 & 0 \\ -i & 0 & 0 & 0 \end{pmatrix} \qquad (1.39)$$

$$\alpha_z = \begin{pmatrix} 0 & 0 & 1 & 0 \\ 0 & 0 & 0 & -1 \\ 1 & 0 & 0 & 0 \\ 0 & -1 & 0 & 0 \end{pmatrix} \qquad \beta = \begin{pmatrix} 1 & 0 & 0 & 0 \\ 0 & 1 & 0 & 0 \\ 0 & 0 & -1 & 0 \\ 0 & 0 & 0 & -1 \end{pmatrix} \qquad (1.40)$$

These matrices can be written in short-hand notation using Pauli matrices.

$$\alpha_i = \begin{pmatrix} 0 & \sigma_i \\ \sigma_i & 0 \end{pmatrix} \qquad \beta = \begin{pmatrix} I & 0 \\ 0 & -I \end{pmatrix} \qquad (1.41)$$

where I is the identity matrix and σ's are the good old Pauli matrices. Substituting the matrices in Schrodinger equation gives us the Dirac equation in momentum basis as follows

$$i\hbar \frac{\partial \Psi}{\partial t} = \left(c \sum_{i=1}^{3} \alpha_i \cdot p_i + \beta mc^2 \right) \Psi \qquad (1.42)$$

By substituting $p \rightarrow i\hbar \partial / \partial x^\mu$, we can obtain the Dirac equation in position space. For the case when $m = 0$ the equation 1.42 is said to be massless Dirac equation. As described in the section Tight Binding Description of Graphene, graphene has a linear energy dispersion near K and K' points therefore the electrons obeys the massless Dirac equation. Moreover, we will work in two-dimension in the calculations because graphene is a two dimensional material. Thus, it is required to emphasis how the Dirac equation explicitly looks in 2D. The α_i matrices in two dimension is nothing but the Pauli spin matrices σ's. Hence,

$$i\hbar \frac{\partial \Psi}{\partial t} = \left[c \begin{pmatrix} \beta mc^2 & p_x - ip_y \\ p_x + ip_y & -\beta mc^2 \end{pmatrix} \right] \Psi \qquad (1.43)$$

The Fermi velocity v_f is the analogue of the speed of light c in graphene. $p = \hbar k$ and the effective mass $m = 0$ in graphene. Then, the bare Hamiltonian becomes

$$H = \hbar v_f \begin{pmatrix} 0 & k_x - \mathrm{i}k_y \\ k_x + \mathrm{i}k_y & 0 \end{pmatrix} \tag{1.44}$$

Notice that this is exactly the same Hamiltonian we found after expanding the tight-binding Hamiltonian around Dirac points.

1.2.0.1. Probability Current for Relativistic Particles

Probability current will be useful while calculating the transition amplitude for a potential barrier so it will be essential to derive here. The derivation of probability current expression for relativistic particles is very similar to the non-relativistic particles'. Thus, let us first derive for non-relativistic particles and then for relativistic particles. We first start with writing down the Schrï¿½dinger's equation:

$$\mathrm{i}\hbar \frac{\partial}{\partial t}\Psi = \frac{-\hbar^2}{2m}\nabla^2\Psi + V\Psi \tag{1.45}$$

Multiply the equation by Ψ^* from left,

$$\mathrm{i}\hbar\Psi^* \frac{\partial}{\partial t}\Psi = \frac{-\hbar^2}{2m}\Psi^*\nabla^2\Psi + \Psi^* V\Psi \tag{1.46}$$

Taking Hermitian conjugate of the equation 1.45, we get

$$-\mathrm{i}\hbar \frac{\partial}{\partial t}\Psi^* = \frac{-\hbar^2}{2m}\nabla^2\Psi^* + V\Psi^* \tag{1.47}$$

Now, we multiply the equation above by Ψ from left,

$$-\mathrm{i}\hbar\Psi \frac{\partial}{\partial t}\Psi^* = \frac{-\hbar^2}{2m}\Psi\nabla^2\Psi^* + \Psi V\Psi^* \tag{1.48}$$

Subtracting 1.48 from 1.46 yields,

$$\mathrm{i}\hbar \left(\Psi^* \frac{\partial\Psi}{\partial t} + \Psi\frac{\partial\Psi^*}{\partial t} \right) = \frac{-\hbar^2}{2m} \left(\Psi^*\nabla^2\Psi - \Psi\nabla^2\Psi^* \right) \tag{1.49}$$

Combining the derivatives gives

$$\mathrm{i}\hbar\frac{\partial|\Psi|^2}{\partial t} \quad = \quad \frac{-\hbar^2}{2m}\left(\Psi^*\nabla^2\Psi - \Psi\nabla^2\Psi^*\right) \tag{1.50}$$

$$= \quad \frac{-\hbar^2}{2m}\nabla\cdot\left(\Psi^*\nabla\Psi - \Psi\nabla\Psi^*\right)$$

By the continuity equation for probability current, we know that

$$-\frac{\partial|\Psi|^2}{\partial t} = \nabla\cdot j \tag{1.51}$$

Hence, the probability current j is obtained as

$$j = \frac{-\hbar}{2m\mathrm{i}}\left(\Psi^*\nabla\Psi - \Psi\nabla\Psi^*\right) \tag{1.52}$$

Now let us follow the same procedure for relativistic particles. We should now write Dirac equation and its Hermitian conjugate:

$$\mathrm{i}\hbar\frac{\partial\Psi}{\partial t} = \left(c\sum_{i=1}^{3}\alpha_i\cdot p_i + \beta mc^2\right)\Psi \tag{1.53}$$

$$-\mathrm{i}\hbar\frac{\partial\Psi^*}{\partial t} = \left(c\sum_{i=1}^{3}\alpha_i\cdot p_i + \beta mc^2\right)\Psi^*$$

Multiplying the first equation from right by Ψ^* and the second equation from left by Ψ gives

$$\mathrm{i}\hbar\Psi^*\frac{\partial\Psi}{\partial t} = \Psi^*\left(c\sum_{i=1}^{3}\alpha_i\cdot p_i + \beta mc^2\right)\Psi \tag{1.54}$$

$$-\mathrm{i}\hbar\Psi\frac{\partial\Psi^*}{\partial t} = \Psi\left(-c\sum_{i=1}^{3}\alpha_i\cdot p_i + \beta mc^2\right)\Psi^*$$

Subtracting the equations above from each other yields

$$\mathrm{i}\hbar\left(\Psi^*\frac{\partial\Psi}{\partial t} + \Psi\frac{\partial\Psi^*}{\partial t}\right) = \Psi^*\left(c\sum_{i=1}^{3}\alpha_i\cdot p_i\right)\Psi + \Psi\left(c\sum_{i=1}^{3}\alpha_i\cdot p_i\right)\Psi^* \tag{1.55}$$

After subtraction, we got rid of the mass term. Then, it is more convenient to switch to position basis for seeing more explicitly.

$$i\hbar\frac{\partial|\Psi|^2}{\partial t} = \frac{\hbar c}{i}\Psi^*\left(\sum_{i=1}^{3}\alpha_i \cdot \nabla_i\right)\Psi + \Psi\left(\sum_{i=1}^{3}\alpha_i \cdot \nabla_i\right)\Psi^* \tag{1.56}$$

Again, by the continuity equation, we obtain the probability current for a relativistic particle as follows:

$$j = c\Psi^*\alpha\Psi \tag{1.57}$$

Sometimes, in literature, σ is used instead of α because α's are Pauli matrices for two-dimension as mentioned previously. Thus, equivalently

$$j = c\Psi^*\sigma\Psi \tag{1.58}$$

1.2.1. Klein Tunneling in Graphene

In chapter 1.1.2, we have seen that in low energy limit the Hamiltonian can be written around K and K' points as

$$H = \hbar v_F k \cdot \hat{\sigma} = \hbar v_F \begin{pmatrix} 0 & k_x - ik_y \\ k_x + ik_y & 0 \end{pmatrix} \tag{1.59}$$

As can easily be seen that this matrix is nothing but the Dirac matrix in two dimension. This fact automatically leads us Klein tunneling in graphene. This is not a surprise because we have shown that the effective mass of electrons in graphene is zero. This means that the electrons behave like photons and they must the obey massless Dirac equation. Let us now consider the potential barrier problem to see Klein tunneling in action. Suppose we have a square potential barrier as in the following figure

We can divide the problem in three zones. Zone 1 is when $x < 0$, zone 2 is when $0 < x < d$ and zone 3 is when $d < x$. The potential can mathematically be written as

$$V(x) = \begin{cases} 0 & \text{if } x \leq 0 \\ V_0 & \text{if } 0 \leq x \leq d \\ 0 & \text{if } d \leq x \end{cases} \tag{1.60}$$
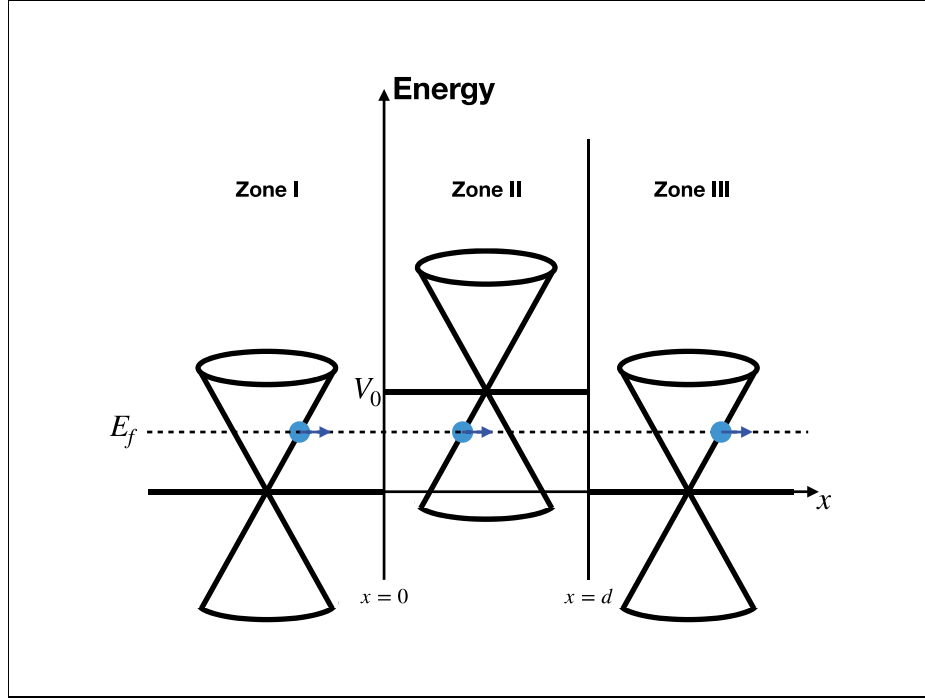
Figure 1.6. The potential regions and corresponding linear energy dispersions.

The Hamiltonian in zone 2 will be $H = \hbar v_F H_{\text{kin}} + V_0 \mathbb{I}$. We already know from chapter 1 the eigenstates of the Hamiltonian as

$$\psi(r) = \begin{pmatrix} 1 \\ \alpha e^{i\phi} \end{pmatrix} e^{ik \cdot r} \tag{1.61}$$

Because our potential is constant in that region, the form of the eigenstates will remain same. Only the wave vector k will be modified to say $q = 2m\sqrt{E - V_0}$. And also the wavevector along y direction is not affected by the potential since the problem has translational symmetry along y direction. The wavefunctions can be found as for three regions

$$\psi_1 = e^{ik_y y} \left[e^{ik_x x} \begin{pmatrix} 1 \\ \alpha e^{i\phi} \end{pmatrix} + r e^{-ik_x x} \begin{pmatrix} 1 \\ -\alpha e^{-i\phi} \end{pmatrix} \right] \tag{1.62}$$

$$\psi_2 = e^{ik_y y} \left[A e^{iqx} \begin{pmatrix} 1 \\ -\alpha e^{-i\theta_A} \end{pmatrix} + B e^{-iqx} \begin{pmatrix} 1 \\ \alpha e^{-i\theta_A} \end{pmatrix} \right] \tag{1.63}$$

$$\psi_3 = t e^{ik_y y} e^{ik_x x} \begin{pmatrix} 1 \\ \alpha e^{i\phi} \end{pmatrix} \tag{1.64}$$
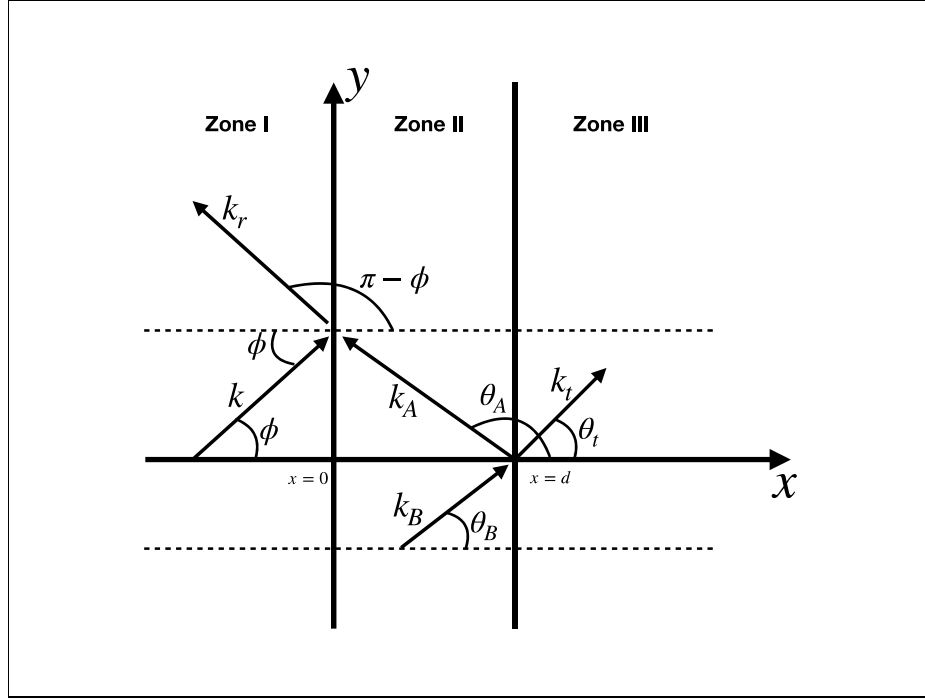
Figure 1.7. Top view of the two dimensional potential barrier.

The wavefunctions must be continuous for potential boundaries $x = 0$ and $x = d$. Applying this boundary condition will give the amplitudes of the ψ's. A nice thing about this condition is that we need only solve for when $\psi_1(0) = \psi_2(0)$ and $\psi_2(d) = \psi_3(d)$ since the wavefunctions come with a spinor. In contrast, we should have considered the continuity of derivatives of the wavefunctions for an ordinary material.

$$1 \quad = \quad -r + A + B \tag{1.65}$$

$$e^{\mathrm{i}\phi} \quad = \quad re^{\mathrm{i}\phi} - Ae^{-\mathrm{i}\theta_A} + Be^{-\mathrm{i}\theta_B} \tag{1.66}$$

$$0 \quad = \quad -te^{\mathrm{i}k_x d} + Ae^{\mathrm{i}qd} + Be^{-\mathrm{i}qd} \tag{1.67}$$

$$0 \quad = \quad -te^{\mathrm{i}\phi}e^{\mathrm{i}k_x d} - Ae^{\mathrm{i}\theta_A}e^{\mathrm{i}qd} + Be^{-\mathrm{i}\theta_A}e^{-\mathrm{i}qd} \tag{1.68}$$

This equation can be written in matrix form.

$$\begin{pmatrix} -1 & 1 & 1 & 0 \\ e^{\mathrm{i}\phi} & -e^{-\mathrm{i}\theta_A} & e^{-\mathrm{i}\theta_B} & 0 \\ 0 & e^{\mathrm{i}k_x d} & e^{-\mathrm{i}q} & -e^{\mathrm{i}d} \\ 0 & -e^{\mathrm{i}(\theta_A + qd)} & e^{-\mathrm{i}(\theta_A + qd)} & -e^{\mathrm{i}(\phi + qd)} \end{pmatrix} \begin{pmatrix} r \\ A \\ B \\ t \end{pmatrix} = \begin{pmatrix} 1 \\ e^{\mathrm{i}\phi} \\ 0 \\ 0 \end{pmatrix} \tag{1.69}$$

The solution of the matrix equation is

$$r = \frac{e^{-\mathrm{i}b}(-1 + e^{2\mathrm{i}d})(e^{\mathrm{i}(2\theta_a + b)} + e^{\mathrm{i}(\theta_a + 2b)} - e^{\mathrm{i}\theta_a} - e^{\mathrm{i}b})}{2e^{\mathrm{i}(\theta_a + b + 2d)} - 2e^{\mathrm{i}(\theta_a + b)} + e^{2\mathrm{i}(\theta_a + b)} + e^{2\mathrm{i}(\theta_a + d)} + 1} \tag{1.70}$$

$$A = -\frac{(1 + e^{2\mathrm{i}b})(-1 + e^{\mathrm{i}a + \mathrm{i}b})}{2e^{\mathrm{i}a + \mathrm{i}b + 2\mathrm{i}d} - 2e^{\mathrm{i}a + \mathrm{i}b} + e^{2\mathrm{i}a + 2\mathrm{i}b} + e^{2\mathrm{i}a + 2\mathrm{i}k_x d} + e^{2\mathrm{i}b + 2\mathrm{i}k_x d} + 1} \tag{1.71}$$

$$B = \frac{(1 + e^{2\mathrm{i}b})(e^{\mathrm{i}a} + e^{\mathrm{i}b})e^{\mathrm{i}a + 2\mathrm{i}k_x d}}{2e^{\mathrm{i}a + \mathrm{i}b + 2\mathrm{i}d} - 2e^{\mathrm{i}a + \mathrm{i}b} + e^{2\mathrm{i}a + 2\mathrm{i}b} + e^{2\mathrm{i}a + 2\mathrm{i}k_x d} + e^{2\mathrm{i}b + 2\mathrm{i}k_x d} + 1} \tag{1.72}$$

$$t = \frac{(1 + e^{2\mathrm{i}a})(1 + e^{2\mathrm{i}b})}{2e^{\mathrm{i}a + \mathrm{i}b + 2\mathrm{i}d} - 2e^{\mathrm{i}a + \mathrm{i}b} + e^{2\mathrm{i}a + 2\mathrm{i}b} + e^{2\mathrm{i}a + 2\mathrm{i}k_x d} + e^{2\mathrm{i}b + 2\mathrm{i}k_x d} + 1} \tag{1.73}$$

The reflection coefficient r can be simplified as following

$$r = \frac{(-2e^{\mathrm{i}\phi} \sin qd)(\sin \phi + sin\theta_A)}{e^{-\mathrm{i}qd} \cos(\phi + \theta_A) + e^{\mathrm{i}qd} \cos(\phi - \theta_A) + 2\mathrm{i} \sin(qd)} \tag{1.74}$$

The transmission coefficient, which we are interested in, can be found by using $T = 1 - |r|^2$ from the probability conservation. After the evaluation, we obtain the transmission probability as

$$T = \frac{\cos^2 \phi \cos^2 \theta_A}{\cos^2 \phi \cos^2(qd) + \sin^2(qd)(1 + \sin \theta_A \sin \phi)^2} \tag{1.75}$$

where $q_x d = -2\pi l \sqrt{1 - 2\epsilon + ep^2 \cos \phi}$ and ϵ is dimensionless energy scale as $\epsilon = E/V_0$ and $l = V_0 d/(2\pi \hbar v_f)$ is the dimensionless barrier width. There are several important cases that can be extracted from the equation 1.75.

1.2.1.1. Zero Incident Angle

The angle $\phi = 0$ for the electrons incoming perpendicularly to the potential barrier. Thus, substituting ϕ into the equation gives 100%. This means that all the electrons passes through the potential barrier regardless of their energy. In figure 1.8, the electrons with different energies are transmitted 100% when $\phi = 0$. This is striking and counter-intuitive results. That is why this tunneling process is also called Klein paradox. This is also the one of the reason that the difficulty of confining electrons in graphene. It is also the reason of high mobility.
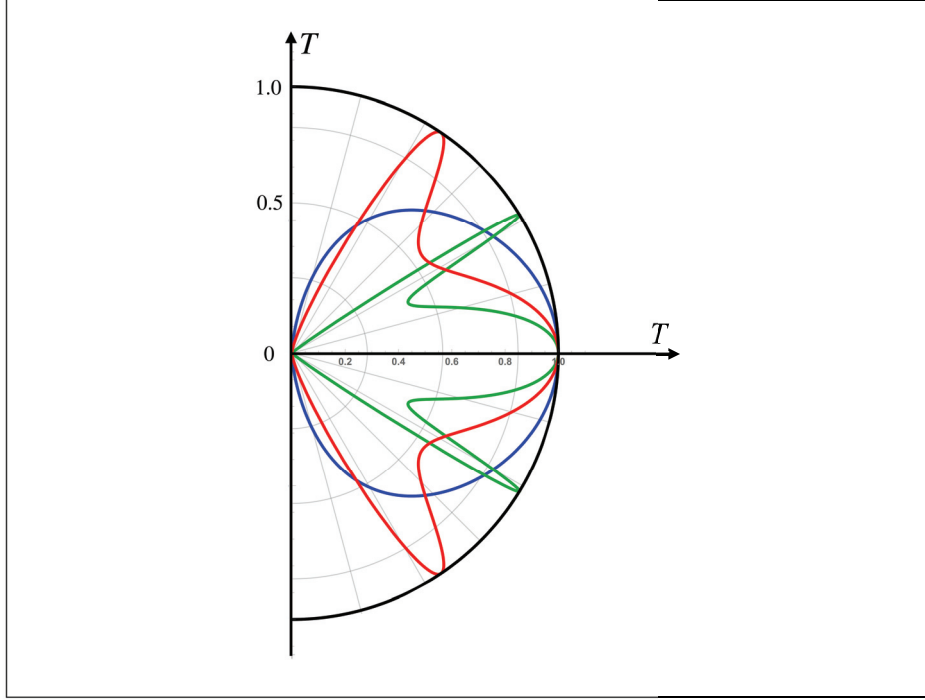
Figure 1.8. The graph of the tunneling probability T on polar coordinates of the incident angle. The black curve represents 100% transmission. Different colors represents different energies of incoming particles ($\epsilon = 0.2$, $l = 2$, blue; $\epsilon = 0.4$, $l = 2$, green; $\epsilon = 0.6$, $l = 2$, red). As can be seen, the transmission rate is 100% if particles come perpendicular to potential barrier. The nodes appeared on different energies correspond to Fabry-Perot resonances.

1.2.1.2. Fabry-Perot Resonances

The form of the potential can be thought as two interferences where are located at $x = 0$ and $x = d$. This causes two scatterings from these interference which can be also thought as a well-known Fabry-Perot interferometer. These scattering gives the nodes in figure 1.8. For different energies, there are different number of nodes. This is because there are larger number of wavelength can fit into the spacing between $x = 0$ and $x = d$. This is another reason that hardens the confinement.

1.2.1.3. Critical Angle

We have defined $\epsilon = E/V_0$ and $q_x d = -2\pi l \sqrt{1 - 2\epsilon + \epsilon^2} \cos\phi$. When the term in the square root becomes less than 0, the x component of the momentum q_x becomes

imaginary. This is an important case because when it becomes imaginary, the plane wave becomes evanescent. This is the case when Klein tunneling is suppressed.
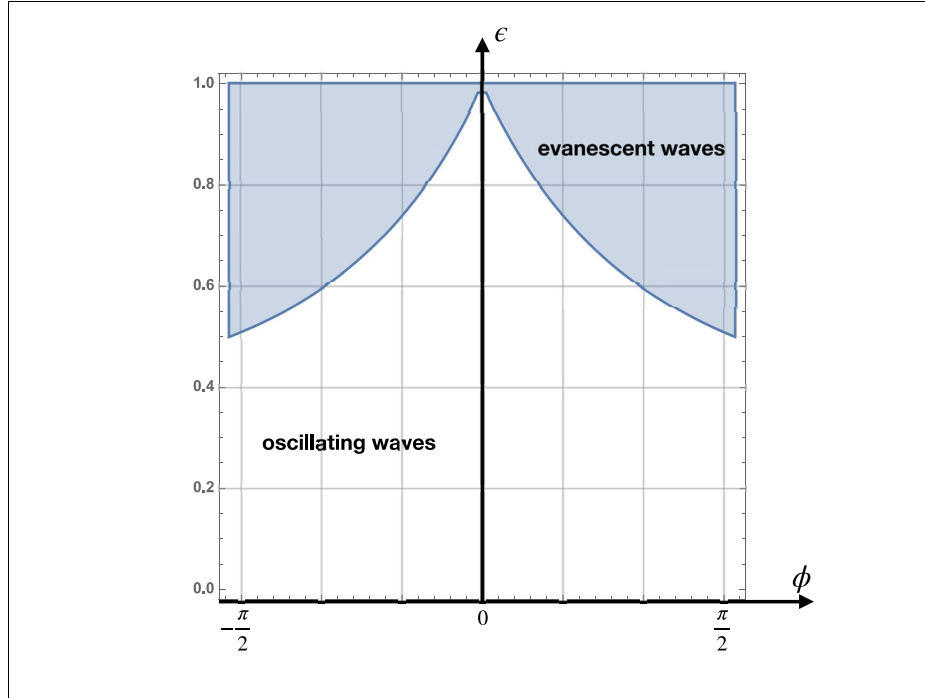
Figure 1.9. The region plot showing the behaviour of the electron wave for the corresponding energy and angle.

$$1 - 2\epsilon + \epsilon^2 \cos\phi < 0 \tag{1.76}$$

When this condition is met, we no longer see Klein tunneling. This will help to confine the electrons in the circular potential well. In figure 1.9, we see the regions when evanescent waves occur. The oscillating waves mean the plane wave of the electrons in graphene. Figure 1.10 summarizes all the relation between energy, incident angle and transmission rate.

1.3. Heisenberg Model

A two-electron system with spin dependency is four-state manifold since spins can take the states: $|\uparrow\uparrow\rangle$, $|\uparrow\downarrow\rangle$, $|\downarrow\uparrow\rangle$, $|\downarrow\downarrow\rangle$. A two-electron system can also be represented by spin singlet and triplet states(Ashcroft and Mermin, 1976). In this case, we should think the electrons as a linear combination of these four states. Our aim is to construct a
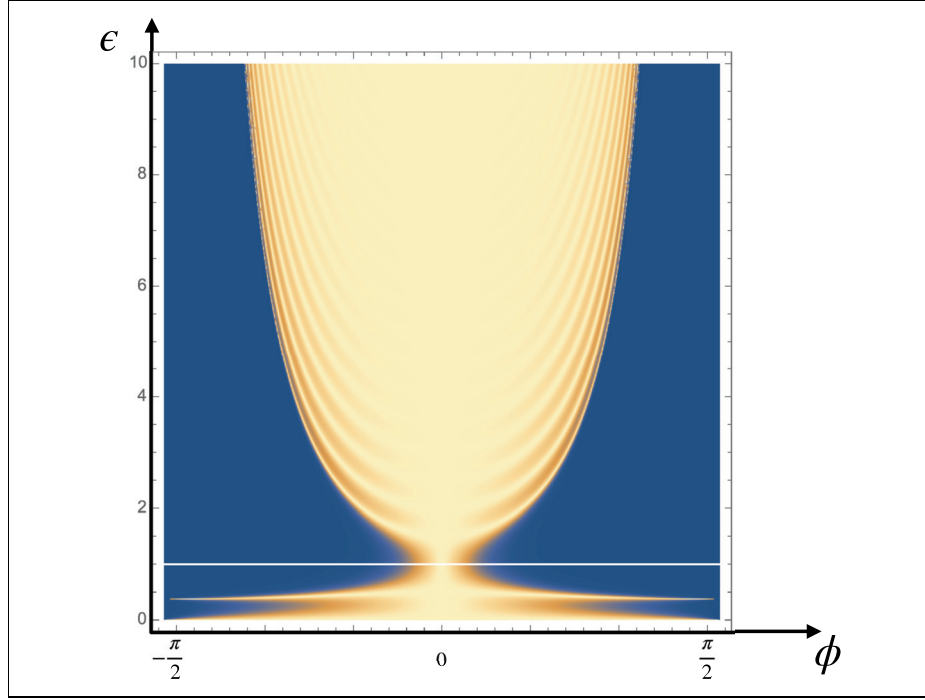
Figure 1.10. The plot of transmission probability T which can be seen in the color code. Yellow parts show the region where the transmission probability is higher.

Hamiltonian which effectively describe the interaction between the spins of the electrons. To achieve this, one must find a Hamiltonian such that its eigenstates are same as the four-state manifold, and eigenvalues are same as the corresponding eigenstates. We know that spin operator for each electron satisfies $\mathbf{S}^2 = S(S+1)\hbar^2 = \frac{1}{2}(\frac{1}{2}+1)\hbar^2 = \frac{3}{4}\hbar^2$

$$\mathbf{S}^2 = (\mathbf{S}_1 + \mathbf{S}_2)^2 = \mathbf{S}_1^2 + \mathbf{S}_2^2 + 2\mathbf{S}_1 \cdot \mathbf{S}_2 = \frac{3}{2} + 2\mathbf{S}_1 \cdot \mathbf{S}_2 \tag{1.77}$$

We now need to calculate action of $\mathbf{S}_1 \cdot \mathbf{S}_2$ on singlet and triplet states.

$$\mathbf{S}_1 \cdot \mathbf{S}_2(|\uparrow\downarrow\rangle - |\downarrow\uparrow\rangle) = (\mathbf{S}_{1x} \cdot \mathbf{S}_{2x} + \mathbf{S}_{1y} \cdot \mathbf{S}_{2y} + \mathbf{S}_{1z} \cdot \mathbf{S}_{2z})(|\uparrow\downarrow\rangle - |\downarrow\uparrow\rangle) \tag{1.78}$$

$$= \frac{\hbar^2}{4}|\downarrow\uparrow\rangle - \frac{\hbar^2}{4}|\uparrow\downarrow\rangle + \frac{\hbar^2}{4}|\downarrow\uparrow\rangle \tag{1.79}$$

$$- \left(\frac{\hbar^2}{4}|\uparrow\downarrow\rangle + \frac{\hbar^2}{4}|\uparrow\downarrow\rangle - \frac{\hbar^2}{4}|\downarrow\uparrow\rangle\right) \tag{1.80}$$

$$= \frac{\hbar^2}{4}(3|\downarrow\uparrow\rangle - 3|\uparrow\downarrow\rangle) \tag{1.81}$$

$$= \frac{-3\hbar^2}{4}(|\uparrow\downarrow\rangle - |\downarrow\uparrow\rangle) \tag{1.82}$$

23

$$\mathbf{S}_1 \cdot \mathbf{S}_2(|\uparrow\downarrow\rangle + |\downarrow\uparrow\rangle) \;\; = \;\; \frac{\hbar^2}{4}|\uparrow\downarrow\rangle + \frac{\hbar^2}{4}|\downarrow\uparrow\rangle - \frac{\hbar^2}{4}|\downarrow\uparrow\rangle + \frac{\hbar^2}{4}|\uparrow\downarrow\rangle + \frac{\hbar^2}{4}|\uparrow\downarrow\rangle - \frac{\hbar^2}{4} \quad (1.83)$$

$$= \;\; \frac{\hbar^2}{4}\left(|\uparrow\downarrow\rangle + |\downarrow\uparrow\rangle\right) \tag{1.84}$$

We have found that the eigenvalues of $\mathbf{S}_1 \cdot \mathbf{S}_2$, $-\frac{3\hbar^2}{4}$ for singlet and $\frac{\hbar^2}{4}$ for triplet state. Finally, we can write the spin operator as

$$H^{\text{spin}} = \frac{1}{4}(E_s + 3E_t) - (E_s - E_t)\mathbf{S}_1 \cdot \mathbf{S}_2 \tag{1.85}$$

where E_s and E_t the energies of singlet and triplet states, respectively. This operator satisfies the desired properties which are $H^{\text{spin}}(|\uparrow\downarrow\rangle - |\downarrow\uparrow\rangle) = -\frac{3}{4}(|\uparrow\downarrow\rangle - |\downarrow\uparrow\rangle)$ and $H^{\text{spin}}(|\uparrow\downarrow\rangle + |\downarrow\uparrow\rangle) = \frac{1}{4}(|\uparrow\downarrow\rangle + |\downarrow\uparrow\rangle)$. The term $\frac{1}{4}(E_s + 3E_t)$ in the spin Hamiltonian can be neglected because it gives nothing but a shift in the energy spectrum. Furthermore, we can define energy difference between singlet and triplet state as J. Hence, the spin Hamiltonian becomes

$$H^{\text{spin}} = -J\mathbf{S}_1 \cdot \mathbf{S}_2 \qquad \text{where } J = E_s - E_t \tag{1.86}$$

One should keep in mind that a system is ferromagnetic when $J > 0$ and antiferromagnetic when $J < 0$. The result can be generalized to N particle system by summing over all spins:

$$H^{\text{spin}} = -\sum_{\text{all spins}} J_{ij}\, \mathbf{S}_i \cdot \mathbf{S}_j \tag{1.87}$$

We have finally obtained the effective Hamiltonian that describes the spin interaction of two particles. This Hamiltonian will be essential to formalize the RKKY interaction.

1.4. RKKY

Exchange interactions can be considered under two categories (Ashcroft and Mermin, 1976). If electrons directly interact with each other using Coulomb interaction, then this type of interactions are called direct exchange. This is often the case when two relatively close magnetic atoms interact due to their overlapping wavefunctions. Another
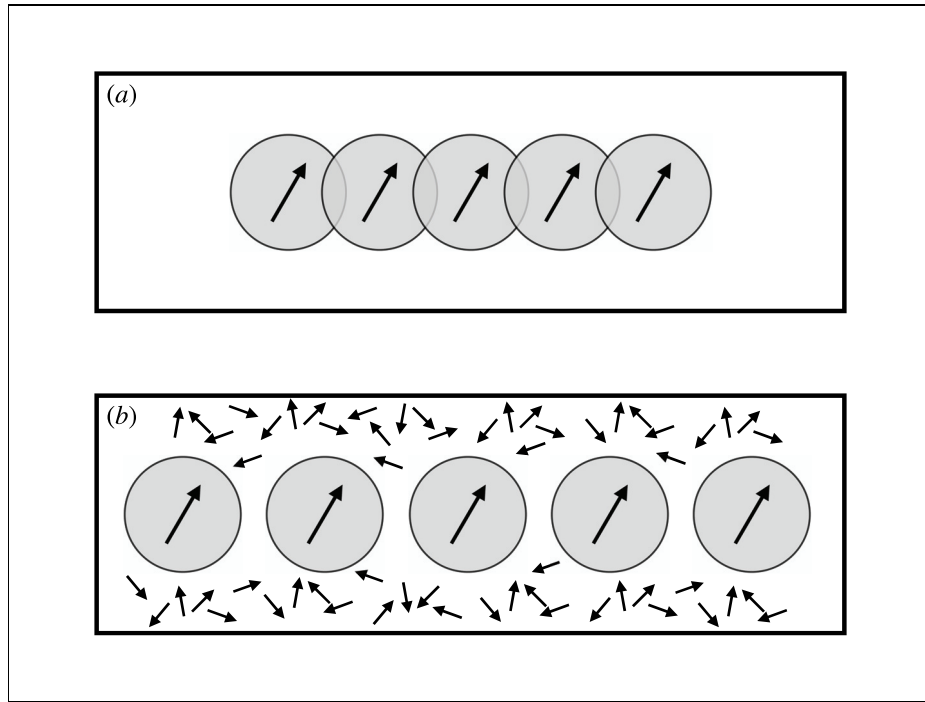
Figure 1.11. Figure (a) shows overlapping wave functions. This is an example of direct exchange. Figure (b), on the other hand, shows distict wave functions where indirect exchange interaction may occur due to the magnetic moments which freely moves in material (Ashcroft and Mermin (1976)).

exchange interaction is indirect exchange because two ions do not directly interact but they interact with the help of conduction electrons.

In this scenario, since ions do not have overlapping wavefunctions, one ion first directly interact with conduction electrons which freely moves in crystal and then the conduction electrons interact with the other ion in the crystal. In the end, two ions in the crystal effectively interact with each other. RKKY interaction lies in the second category. This is why often stated as RKKY interaction is an indirect interaction mediated by conduction electrons (Kittel, 1963).

The name of RKKY comes from the physicists Ruderman-Kittel-Kasuya-Yosida. RKKY interaction describes two closely related phenomena in metals. One is the indirect interaction of two nuclear magnetic moments via their hyperfine interaction with the conduction electrons, and the other is the magnetic moment of ions with again the conduction electrons. In this thesis, we are interested in the second type of mechanism so the interaction between nuclear moments is ignored. The second mechanism can be thought in Heisenberg model framework as discussed in previous chapter. These spin-spin interactions can be written as a Heisenberg type Hamiltonian as follows (Nolting and

Ramakanth, 2009).
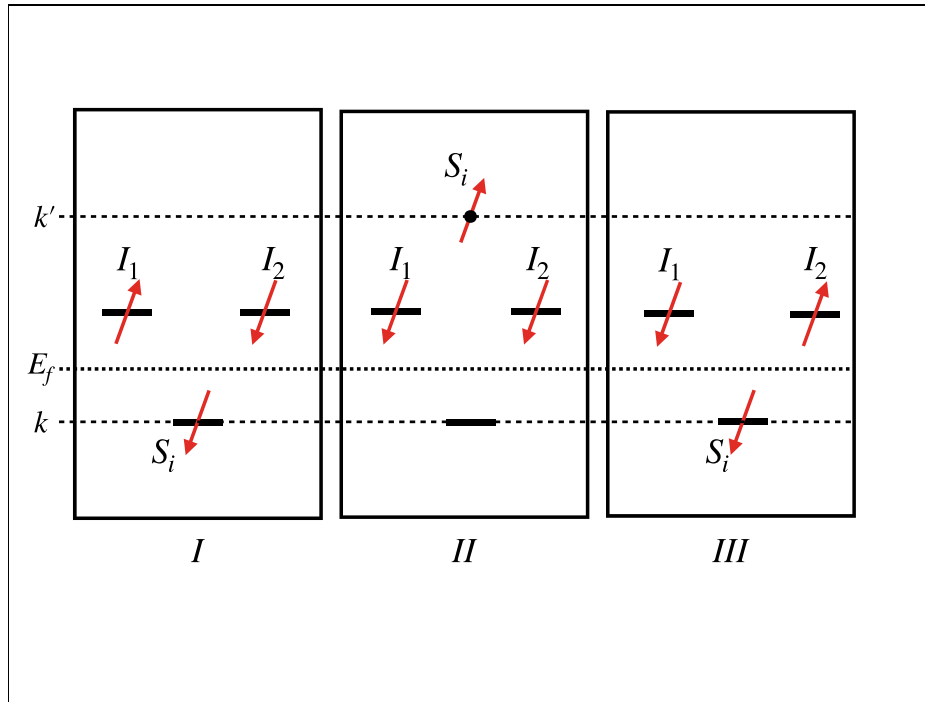
Figure 1.12. Figure shows that two localized magnetic moments I_1 and I_2, and a magnetic moment of conduction electrons S_i. In I, S_i interact with I_1 by exchanging their spins and scatter to k' state from k state. In II, S_i moves in material and exchange its spin with I_2. In III, S_i turns back its originial state k but in the end I_1 and I_2 exchange their spins.

$$H = \sum_i J_{1i} I_1 \cdot S_i + J_{2i} I_2 \cdot S_i \tag{1.88}$$

where I's are the localized magnetic moments and S_i's are the spin of the conduction electrons. J_{1i} and J_{2i} are the coupling constants between the magnetic moments and the conduction electrons. RKKY theory states that, by using second order perturbation, the Heisenberg type Hamiltonian can be effectively written as an interaction between two localized moments with a coupling constant J_{RKKY}. Mathematically:

$$H = \sum_i J_{1i} I_1 \cdot S_i + J_{2i} I_2 \cdot S_i \quad \longrightarrow \quad H_{\text{RKKY}} = \sum_i J_{\text{RKKY}} I_1 \cdot I_2 \tag{1.89}$$

Let us now explicitly show how we obtain 1.89. Suppose that we have two magnetic moments placed at R_i and R_j and they are not directly coupled. We can write the Hamiltonian for conduction electrons as

$$H = \sum_{k,\sigma} \epsilon(k) c_{k\sigma}^{\dagger} c_{k\sigma} \tag{1.90}$$

where k, σ is the wavevector and spin of the conduction electrons. $c_{k\sigma}$ and $c_{k\sigma}^{\dagger}$ are annihilation and creation operators, respectively. The interaction term (left hand side of the equation 1.89) can be written in terms of spin operators. For simplicity assume that coupling constants are same for two magnetic moments so $J_{1i} = J_{2i} = J$.

$$H_{\text{int}} = -J \sum_{i=1}^{2} S_i \cdot I_i = -J \sum_{i=1}^{2} \left[S_i^z I_i^z + \frac{1}{2}(S_i^+ I_i^- + S_i^- I_i^+) \right] \tag{1.91}$$

The spin operators can be written in terms of creation and annihilation operators.

$$S_i^z = \frac{\hbar}{2} \left(c_{i\uparrow}^{\dagger} c_{i\uparrow} - c_{i\downarrow}^{\dagger} c_{i\downarrow} \right) \tag{1.92}$$

$$S_i^+ = \hbar\, c_{i\uparrow}^{\dagger} c_{i\downarrow} \tag{1.93}$$

$$S_i^- = \hbar\, c_{i\downarrow}^{\dagger} c_{i\uparrow} \tag{1.94}$$

Since c and $c^{\dagger}$ are the annihilation and creation operators of electrons, they satisfy the following Fermionic commutation relations:

$$\{c_{i\sigma}, c_{j\sigma'}\} = \{c_{i\sigma}^{\dagger}, c_{j\sigma'}^{\dagger}\} = 0 \tag{1.95}$$

$$c_{i\sigma}^2 = (c_{i\sigma}^{\dagger})^2 = 0 \tag{1.96}$$

$$\{c_{i\sigma}, c_{j\sigma'}^{\dagger}\} = \delta_{ij}\delta_{\sigma\sigma'} \tag{1.97}$$

Using Fourier transformation, c and $c^{\dagger}$ can be written in momentum space

$$c_{i\sigma} = \frac{1}{\sqrt{N}} \sum_q e^{iq \cdot R_i} c_{q\sigma} \tag{1.98}$$

$$c_{i\sigma}^{\dagger} = \frac{1}{\sqrt{N}} \sum_q e^{-iq \cdot R_i} c_{q\sigma}^{\dagger} \tag{1.99}$$

$$\tag{1.100}$$

The interaction term then becomes in momentum space

$$H_{\text{int}} = -\frac{J\hbar}{2N} \sum_i \sum_{k,q} e^{-iq \cdot R_i} \left[I_i^z \left(c_{q+k,\uparrow}^\dagger c_{k,\uparrow} - c_{q+k,\downarrow}^\dagger c_{k\downarrow} \right) \right.$$

$$\left. + I_i^+ c_{k+q,\downarrow}^\dagger c_{k,\uparrow} + I_i^- c_{k+q,\uparrow}^\dagger c_{k,\downarrow} \right] \quad (1.101)$$

Notice that we are not including the spin-orbit coupling. Thus, we can separate the spin and position space since they are not mixed. We now treat the interaction term as perturbation and find the energies. From perturbation theory, the first order correction is

$$E_0^{(1)} = \langle 0 | H_{\text{int}} | 0 \rangle \quad (1.102)$$

the first order term does not contribute because

$$\langle 0 | I_i^- c_{k+q,\uparrow}^\dagger c_{k,\downarrow} | 0 \rangle = 0 \quad (1.103)$$

$$\langle 0 | I_i^+ c_{k+q,\downarrow}^\dagger c_{k,\uparrow} | 0 \rangle = 0 \quad (1.104)$$

$$\langle 0 | - I_i^z c_{q+k,\downarrow}^\dagger c_{k\downarrow} | 0 \rangle = 0 \quad (1.105)$$

$$\langle 0 | I_i^z c_{q+k,\uparrow}^\dagger c_{k,\uparrow} | 0 \rangle = 0 \quad (1.106)$$

Hence, we should consider the second order corrections using the following expression

$$E_0^{(2)} = \sum_{(A,f) \neq (0,f)} \frac{|\langle 0, f | H_{\text{int}} | A, f' \rangle|^2}{E_0^{(0)} - E_A^{(0)}} \quad (1.107)$$

where A is an excited eigenstate of an unpertubed system with corresponding energy $E_A^{(0)}$. Define Heaviside function as follows:

$$\theta = \begin{cases} 1 & x > 0 \\ 0 & x < 0 \end{cases} \quad (1.108)$$

Then we can write

$$\theta_{k,k'} = \theta(k_f - k')\theta(k - k_f) \quad (1.109)$$

which guarantees that $k(k')$ is under (above) the Fermi level. We have

$$\langle k'm_s| c_{k'\uparrow}^\dagger c_{k\downarrow} |km_s\rangle \quad\longrightarrow\quad \theta_{k,k'}\frac{1}{\hbar}\langle m_s'| s_+ |m_s\rangle \tag{1.110}$$

$$\langle k'm_s| c_{k'\downarrow}^\dagger c_{k\uparrow} |km_s\rangle \quad\longrightarrow\quad \theta_{k,k'}\frac{1}{\hbar}\langle m_s'| s_- |m_s\rangle \tag{1.111}$$

and the energy difference in the denominator of the expression becomes

$$E_0^{(0)} - E_{(0)} = \epsilon(k') - \epsilon(k) \tag{1.112}$$

Finally we can write the expression as follows:

$$E_0^{(2)} = \frac{J^2}{4N^2}\sum_{k,k'}\frac{\theta_{k,k'}}{\epsilon(k')-\epsilon(k)}\sum_{i,j}\sum_{m_s',m_s}\sum_{f'} e^{-\mathrm{i}(k-k')\cdot(R_i-R_j)} \tag{1.113}$$

$$\times\quad \langle f| 2I_i^z \langle m_s'| s_z |m_s\rangle + I_i^+ \langle m_s'| s_- |m_s\rangle + I_j^- \langle m_s'| s_+ |m_s\rangle |f'\rangle \tag{1.114}$$

$$\times\quad \langle f'| 2I_j^z \langle m_s'| s_z |m_s\rangle + I_j^+ \langle m_s'| s_- |m_s\rangle + I_j \langle m_s'| s_+ |m_s\rangle |f\rangle \tag{1.115}$$

We can get rid of the terms containing $|m_s'\rangle$ and $|f'\rangle$ using the following completeness relations.

$$\sum_{f'} |f'\rangle \langle f'| = 1 \qquad\qquad \sum_{m_s'} |m_s'\rangle \langle m_s'| = 1 \tag{1.116}$$

We obtain

$$E_0^{(2)} = \frac{J^2}{4N^2}\sum_{k,k'}\sum_{i,j}\theta_{k,k'}\frac{e^{-\mathrm{i}(k-k')\cdot(R_i-R_j)}}{\epsilon(k')-\epsilon(k)}\langle f| 2I_i^z I_j^z + I_i^\dagger I_j^- + I_i^- I_j^+ |f\rangle \tag{1.117}$$

The expression above can simple be written as

$$E_0^{(2)} = \frac{J^2}{4N^2}\sum_{k,k'}\sum_{i,j}\theta_{k,k'}\frac{e^{-\mathrm{i}(k-k')\cdot(R_i-R_j)}}{\epsilon(k')-\epsilon(k)}\langle f| I_i \cdot I_j |f\rangle \tag{1.118}$$

As promised in the beginning, the second order energy correction above can be thought as the eigenvalue of an effective Heisenberg type Hamiltonian:

$$H^{\mathrm{RKKY}} = -\sum_{i,j} J_{i,j}^{\mathrm{RKKY}} I_i \cdot I_j \tag{1.119}$$

where the coupling constant J is

$$J_{i,j}^{\text{RKKY}} = -\frac{J^2\hbar^2}{2N^2} \sum_{k,k'} \sum_{i,j} \theta_{k,k'} \frac{e^{-\mathrm{i}(k-k')\cdot(R_i-R_j)}}{\epsilon(k') - \epsilon(k)} \tag{1.120}$$

Here, $\theta_{k,k'}$ represents the occupation of states with momentum k and k'. In this thesis, we used $n_k(1 - n_{k'})$ instead where n_k represents the occupation of a state with momentum k.

CHAPTER 2

METHODS

Along with tight binding model, we used three different techniques to calculate the exchange interaction. Hubbard Mean Field model is used for calculating the exchange interaction in the zigzag-edged graphene nanoflakes. Exact diagonalization and the integral expansion methods are used for calculating the exchange interaction for materials with quartic dispersion.

2.1. Hubbard Mean Field Model

Hubbard model is used to find magnetism by adding a simple term to the tight binding model (Marder, 2010; Ashcroft and Mermin, 1976).

$$H = -t \sum_{<i,j>\sigma} \left(c_i^\dagger c_j + h.c. \right) + U \sum_i n_{i\uparrow} n_{i\downarrow} \tag{2.1}$$

here t is the hopping parameter and n's are the number operators. U is a constant and often called as Hubbard U term. U is the amount of energy acquired to add one more electron to the atomic site. One should keep in mind that U is positive so it gives a repulsive contribution. The mean field method is handy tool to solve an Hamiltonian like above. We can write the number operators as follows:

$$n_{i\uparrow} = (n_{i\uparrow} - \langle n_{i\uparrow} \rangle) + \langle n_{i\uparrow} \rangle \tag{2.2}$$

$$n_{i\downarrow} = (n_{i\downarrow} - \langle n_{i\downarrow} \rangle) + \langle n_{i\downarrow} \rangle \tag{2.3}$$

We added and subtracted $\langle n_{i\uparrow} \rangle$ ($\langle n_{i\downarrow} \rangle$) from $n_{i\uparrow}$ ($\langle n_{i\downarrow} \rangle$). By doing this we could interpret the term in the paranthesis as the fluctuation of number of up-spin (down-spin) electrons from the average number of up-spin (down-spin) electrons. In the end, we assume that this fluctuation is very small and we will get rid of some cross term. This will ease the problem because the difficulty of the problem arises from the multiplication of two number operators. As well-known the number operators are $n = c^\dagger c$ and it is difficult to deal with the multiplication of four field operators. However, one needs to be careful

while using mean-field because if the system has large fluctuations the model will not work at all. Then, we can write the second part of the Hamiltonian as

$$n_{i\uparrow}n_{i\downarrow} = (n_{i\uparrow} - \langle n_{i\uparrow}\rangle) + \langle n_{i\uparrow}\rangle)((n_{i\downarrow} - \langle n_{i\downarrow}\rangle) + \langle n_{i\downarrow}\rangle) \qquad (2.4)$$

$$= (n_{i\uparrow} - \langle n_{i\uparrow}\rangle)(n_{i\downarrow} - \langle n_{i\downarrow}\rangle) + (n_{i\uparrow} - \langle n_{i\uparrow}\rangle)\langle n_{i\downarrow}\rangle \qquad (2.5)$$

$$+ \langle n_{i\uparrow}\rangle(n_{i\downarrow} - \langle n_{i\downarrow}\rangle) + \langle n_{i\uparrow}\rangle\langle n_{i\downarrow}\rangle \qquad (2.6)$$

The trick is to assume that the deviation of $n_{i\uparrow}$ ($n_{i\downarrow}$) from $\langle n_{i\uparrow}\rangle$ ($\langle n_{i\downarrow}\rangle$) is very small. Thus, we can neglect the term $(n_{i\uparrow} - \langle n_{i\uparrow}\rangle)(n_{i\downarrow} - \langle n_{i\downarrow}\rangle)$ because the multiplication of two small quantities is even smaller. Then we have

$$n_{i\uparrow}n_{i\downarrow} = (n_{i\uparrow} - \langle n_{i\uparrow}\rangle)\langle n_{i\downarrow}\rangle + \langle n_{i\uparrow}\rangle(n_{i\downarrow} - \langle n_{i\downarrow}\rangle) + \langle n_{i\uparrow}\rangle\langle n_{i\downarrow}\rangle \qquad (2.7)$$

$$= n_{i\uparrow}\langle n_{i\downarrow}\rangle - \langle n_{i\uparrow}\rangle\langle n_{i\downarrow}\rangle + \langle n_{i\uparrow}\rangle n_{i\downarrow} - \langle n_{i\uparrow}\rangle\langle n_{i\downarrow}\rangle + \langle n_{i\uparrow}\rangle\langle n_{i\downarrow}\rangle \qquad (2.8)$$

$$= n_{i\uparrow}\langle n_{i\downarrow}\rangle + \langle n_{i\uparrow}\rangle n_{i\downarrow} - \langle n_{i\uparrow}\rangle\langle n_{i\downarrow}\rangle \qquad (2.9)$$

In the end, we have got rid of the multiplication of two number operators. By substituting what we found into the Hamiltonian yields

$$H = -t\sum_{<i,j>\sigma}\left(c_i^\dagger c_j + h.c.\right) + U\sum_i (n_{i\uparrow}\langle n_{i\downarrow}\rangle + \langle n_{i\uparrow}\rangle n_{i\downarrow} - \langle n_{i\uparrow}\rangle\langle n_{i\downarrow}\rangle) \qquad (2.10)$$

We have terms like averages of number operators in the Hamiltonian. To calculate them, we initially assign random spins orientation for all spins in the system. Then, we diagonalize the Hamiltonian and calculate the respective averages and feed them into the Hamiltonian in the next iteration. We get a convergence of these averages after many recursive iterations. We finally obtain a Hamiltonian that will be used in the RKKY calculations.

2.2. Exact Diagonalization

Exact diagonalization is a technique to calculate indirect exchange interaction without using any perturbation. In this case, we start with the same tight-binding Hamiltonian with Heisenberg type spin-spin interaction term.

$$H = -t_1 \sum_{<i,j>} c_i^\dagger c_j - t_2 \sum_{<<i,j>>} c_i^\dagger c_j + \sum_{i,j} J_{ij}\, I_i\, S_j \qquad (2.11)$$

In this method, we think of the Hamiltonian as $2n \times 2n$ matrix as follows.

$$\begin{pmatrix} H_\uparrow & H_{\uparrow\downarrow} \\ H_{\downarrow\uparrow} & H_\downarrow \end{pmatrix}_{2n \times 2n} \qquad (2.12)$$

$H_\uparrow$ and $H_\downarrow$ are same with our tight-binding Hamiltonian, and the off-diagonal terms $H_{\uparrow\downarrow}$ and $H_{\downarrow\uparrow}$ describes the coupling between spin-up and spin-down at i^{th} and j^{th} lattice sites. The off-diagonal terms are really sparse. They only contain few terms. We can obtain all the required information about the system by diagonalizing the Hamiltonian. RKKY interaction can be extracted from this Hamiltonian as well. We first align the impurities in ferromagnetic configuration (FM) and so does for antiferromagnetic configuration (AFM) (Black-Schaffer, 2010b; Deaven et al., 1991). The energy difference between the configurations gives the exchange coupling J.

Let $|I_1 I_2\rangle$ shows the spin state of the magnetic moments at 1 and 2. Then, suppose that we have ferromagnetic configuration as $|\uparrow\uparrow\rangle$ and anti-ferromagnetic configuration $|\uparrow\downarrow\rangle$. The corresponding energies can be found as

$$S_1 \cdot S_2 |\uparrow\uparrow\rangle \;=\; \frac{\hbar^2}{4} |\downarrow\downarrow\rangle - \frac{\hbar^2}{4} |\downarrow\downarrow\rangle + \frac{\hbar^2}{4} |\uparrow\uparrow\rangle = \frac{\hbar^2}{4} |\uparrow\uparrow\rangle \qquad (2.13)$$

$$S_1 \cdot S_2 |\uparrow\downarrow\rangle \;=\; \frac{\hbar^2}{4} |\downarrow\uparrow\rangle - \frac{\hbar^2}{4} |\downarrow\uparrow\rangle - \frac{\hbar^2}{4} |\downarrow\uparrow\rangle = -\frac{\hbar^2}{4} |\downarrow\uparrow\rangle$$

Then the energy difference between ferromagnetic and anti-ferromagnetic configurations is $\frac{\hbar^2}{2}$. It is also discussed that the coupling J is the energy difference between the singlet and triplet configurations in Section 1.3 about Heisenberg Model. J is defined as the energy difference between the singlet and triplet states which was $\frac{\hbar^2}{2}$. This is exactly same as the energy difference between antiferromagnetic and ferromagnetic energy difference. One should be careful that we only considered $|\downarrow\uparrow\rangle$. There is one more possibility which is $|\uparrow\downarrow\rangle$. Thus, we should multiply the difference by 2. Finally, the indirect exchange coupling J becomes

$$J = \frac{\text{E(FM)-E(AFM)}}{2} \qquad (2.14)$$

33

To sum up, we write two Hamiltonians for spin-up and spin-downs. Then finding corresponding energies by diagonalizing the Hamiltonians. The energy difference gives us the RKKY interaction strength J.

2.3. Integral Expansion for Quartic Dispersion Calculations

In quartic calculation part, we used four different methods to cross-check. We used integral expansion, tight-binding, exact diagonalization and Green's function methods. Integral expansion is the method that we only used in the calculation of quartic dispersion. We know that, using second order perturbation, RKKY interaction can be written as

$$J = J_1 J_2 \sum_{\substack{k,k' \\ i \neq j}} \frac{\Psi_k(R_i)\Psi_{k'}^*(R_i)\Psi_{k'}(R_j)\Psi_k^*(R_j)}{\epsilon_k - \epsilon_{k'}} \, n_k(1 - n_{k'}) \tag{2.15}$$

where ϵ is the energy and $\Psi_k(R_i)$ is the wave function at R_i with momentum k. In the continuous limit, the wave function are plane waves and the effective Hamiltonian takes the following form

$$J = J_1 J_2 \int \mathrm{d}^2k \mathrm{d}^2k' \frac{e^{\mathrm{i}(k-k')\cdot R_1} e^{-\mathrm{i}(k-k')\cdot R_2}}{\epsilon - \epsilon'} \tag{2.16}$$

We can change basis to polar coordinates and write plane waves in terms of Bessel functions $J_0(k)$. Define $R \equiv R_1 - R_2$ and assign $k := kR$ and $k' := k'R$.

$$J = J_1 J_2 \int \mathrm{d}^2k \mathrm{d}^2k' \frac{J_0(k)J_0(k')}{-\alpha(k^4 - k'^4)} \tag{2.17}$$

$$= -J_1 J_2 \frac{2\pi}{\alpha} \int \mathrm{d}k' k' \int \mathrm{d}k k \frac{J_0(k)J_0(k')}{k^4 \left(1 - \frac{k'^4}{k^4}\right)}$$

$$\tag{2.18}$$

$$= -J_1 J_2 \frac{2\pi}{\alpha} \int_0^{k_f} \mathrm{d}k' k' \int_{k_f}^{\infty} \mathrm{d}k \frac{1}{k^3} J_0(k)J_0(k') \sum_{n=0}^{\infty} \left(\frac{k'}{k}\right)^{4n}$$

$$= \frac{-2\pi J_1 J_2}{\alpha} \sum_{n=0}^{\infty} \left[\int_0^{k_f} \mathrm{d}k' k' \int_{k_f}^{\infty} \mathrm{d}k \frac{1}{k^3} J_0(k) J_0(k') \left(\frac{k'}{k} \right)^{4n} \right] \tag{2.19}$$

$$= \frac{-2\pi J_1 J_2}{\alpha} \sum_{n=0}^{\infty} \left[\int_0^{k_f} \mathrm{d}k' k'^{4n+1} J_0(k') \int_{k_f}^{\infty} \mathrm{d}k k^{-4n-3} J_0(k) \right]$$

Reassigning $kR := k$ and $k'R := k'$ gives

$$J = \frac{-2\pi J_1 J_2}{\alpha} \sum_{n=0}^{\infty} \left[\int_0^{k_f R} \mathrm{d}k' k'^{4n+1} J_0(k') \int_{k_f R}^{\infty} \mathrm{d}k k^{-4n-3} J_0(k) \right] \tag{2.20}$$

Here we have an infinite sum over n which is not practical to evaluate. Thus, we tried the sum for different n values and found that the integral is convergent and it is sufficient to take $n = 50$.
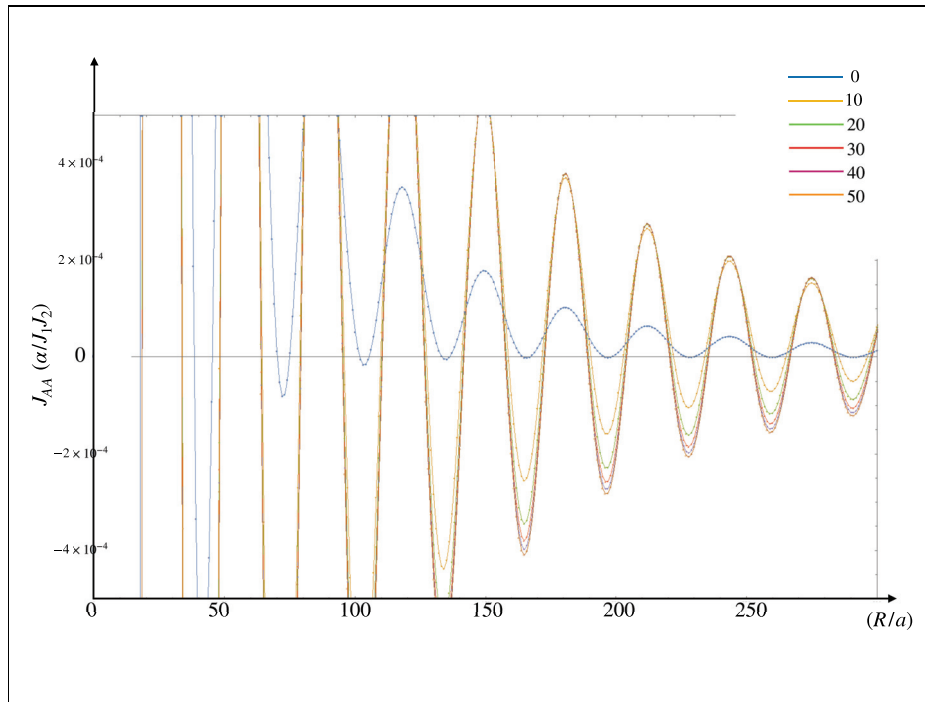
Figure 2.1. Integral expansion in different orders. Graph shows the integral converges
as the expansion order increases.

CHAPTER 3

RKKY INTERACTION UNDER CIRCULAR POTENTIAL

In this chapter, we first calculate the RKKY interaction for bulk graphene and then we calculate the interaction for applied circular potential.

3.1. RKKY Interaction in Bulk Graphene

We calculate the RKKY interaction for bulk graphene. By bulk graphene, we mean that infinite sheet of monolayer graphene. We used exact diagonalization method mentioned in section 2. We take 22500 atoms to calculate the interaction. We used periodic boundary condition to simulate infinite sheet. We put one magnetic moment at center of the system and moved another moment along zigzag and armchair directions for both same and different sublattices.

Figure 3.1. RKKY interaction between the magnetic moments on the same sublattices (J_{AA}) in bulk graphene along zigzag direction.

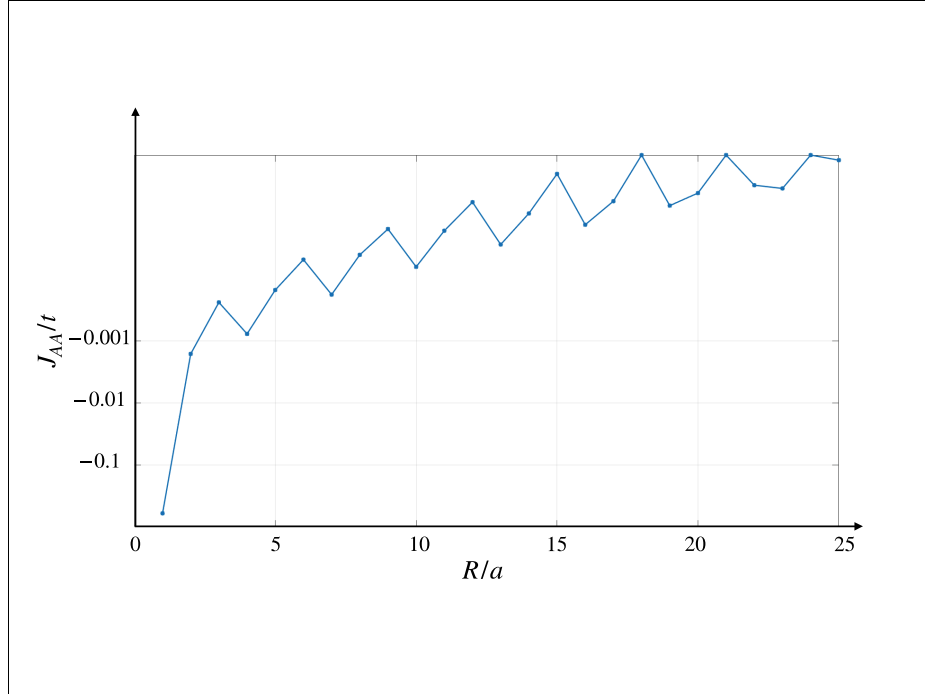We calculated the interaction strength for each increment of movement which will give us the interaction strength as a function of distance between the magnetic moments. We found that the results have a great agreement with the results in literature (Black-Schaffer, 2010a; Saremi, 2007; Black-Schaffer, 2010b; **?**; Power and Ferreira, 2013). It can be seen in figures 3.1 that the RKKY interaction for the magnetic moments located at same sublattices J_{AA} is ferromagnetic. The interaction strength exhibits $1/R^3$ decay behaviour where R is the distance between the magnetic moments. For zigzag direction, there are oscillations in the order of lattice parameter. By using lattice Green's function for bulk graphene, J_{AA} can be found as following Sherafati and Satpathy (2011)

$$J_{AA} = -\frac{9J_1 J_2 \hbar^2}{256\pi t} \times \frac{1 + \cos[(K - K') \cdot R]}{(R/a)^3} \tag{3.1}$$

where J_1 and J_2 coupling constants between the spin of electrons and the localized magnetic moments; K and K' are the vectors indicating the Dirac points in the Brillouin zone. The oscillations are coming from the term including cosine. For armchair direction, the cosine term will vanish so does the oscillations. This behaviour is verified by our tight binding model.
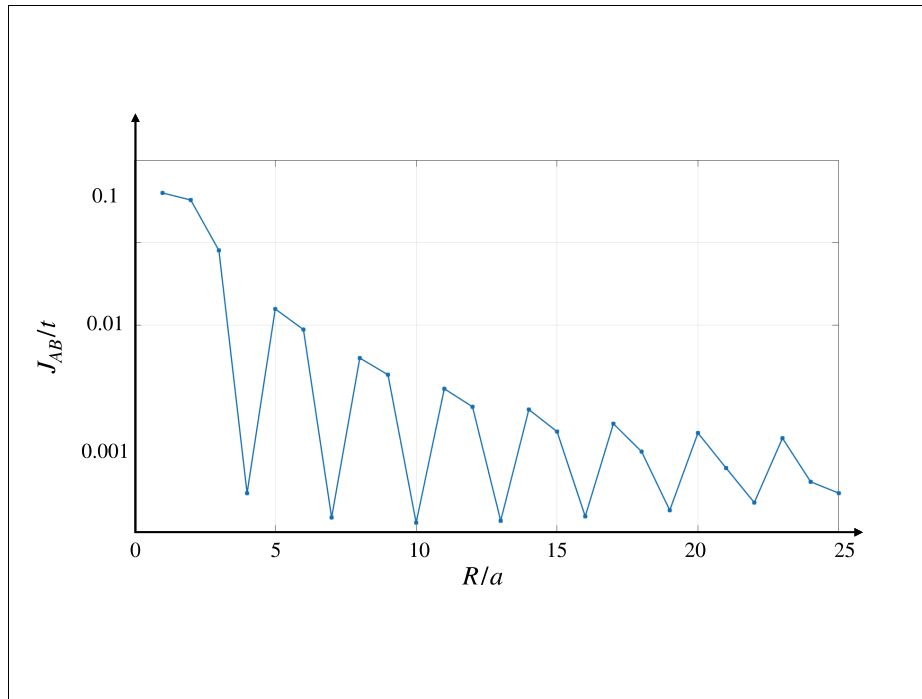

Figure 3.2. RKKY interaction between the magnetic moments on the different sublattices (J_{AB}) in bulk graphene along zigzag direction.
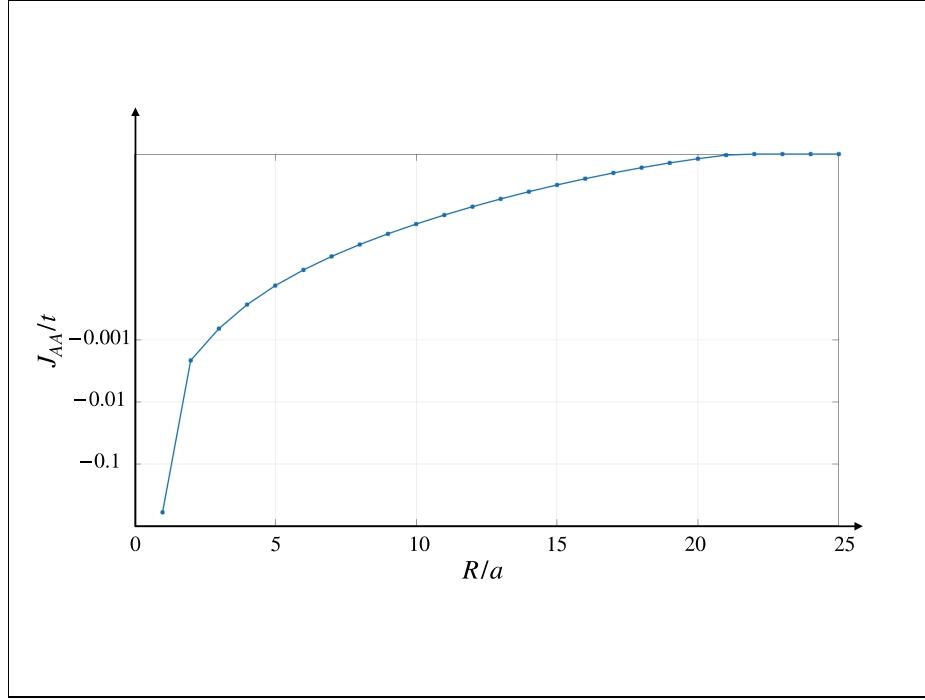
Figure 3.3. RKKY interaction between the magnetic moments on the same sublattices (J_{AA}) in bulk graphene along armchair direction.

3.2.   RKKY Interaction under Applied Circular Potential

In the beginning, we claimed that RKKY interaction can be enhanced via quasi-bound states formed in an applied potential. We again used tight-binding method to test this idea. We took 22500 atoms in this case and apply smoothly varying sigmoid potential whose depth is the quarter of the hopping parameter. The potential is at the center of the system and the radius is $30a$ where a is the distance between the carbon atoms. Because it is not practical to plot all the atoms, figure 3.5, shows a small version of the system we dealt with.

Sigmoid function is nothing but the well-known Fermi distribution function. In two dimension, it takes the form of $f(x) = 1/(e^{\sigma \sqrt{x^2+y^2}} + 1)$ We chose this potential because it is quite similar to the two-dimensional Heaviside potential. The choice of the potential function is extremely important because it is more physical and also one cannot achieve confinement in the potential region due to Klein tunneling. That is the reason why we choose smoothly varying potential. We determined radius of the potential as $30a$. By the radius, we mean that the half maximum of the potential.

In the absence of the circular potential, there are quasi bound states formed in
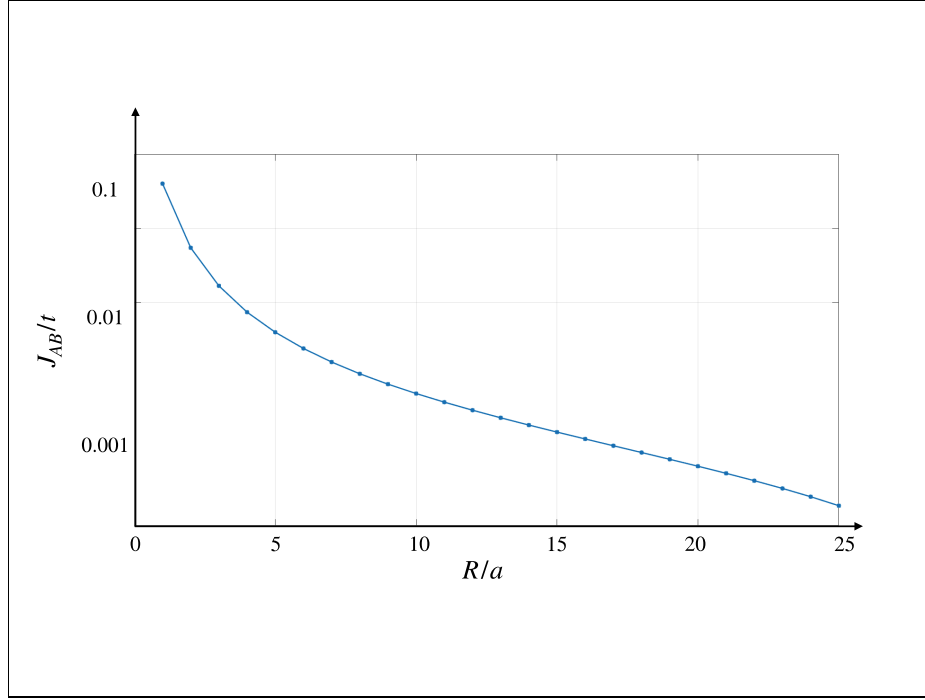
Figure 3.4. RKKY interaction between the magnetic moments on the different sublattices (J_{AB}) in bulk graphene along armchair direction.

the potential region. Those states can be seen in the local density of states graph 3.2. Each peak corresponds to an increase in the number of states within the potential region. Figure 3.2 and 3.2 show an confined electron mode in the potential region. The RKKY interaction is enhanced via these confined states.

To calculate the RKKY interaction, we first fix the position of a magnetic moment at the edge of the sigmoid potential. Then, we move other magnetic moment along the edge and calculate the strength of RKKY interaction as a function of the angle between them.

It would be computationally costly to map entire system therefore it is more practical to calculate the exchange energy on the edge of the potential well. However, this cause some noise in the data which can be seen in the figure 3.2 because the confined modes are not uniformly distributed in the potential region. Thus, the sharp changes in the wavefunctions lying near Fermi level cause the oscillation in the RKKY interaction calculation.

Figure 3.2 compares RKKY interaction with bulk graphene and the system we are concerning. As the angle increase, the RKKY strength decreases for bulk graphene. Notice that it does not decay as $1/R^3$ because we are plotting as a function of the angle. Blue lines represents the RKKY interaction for the sigmoid potential case and the RKKY
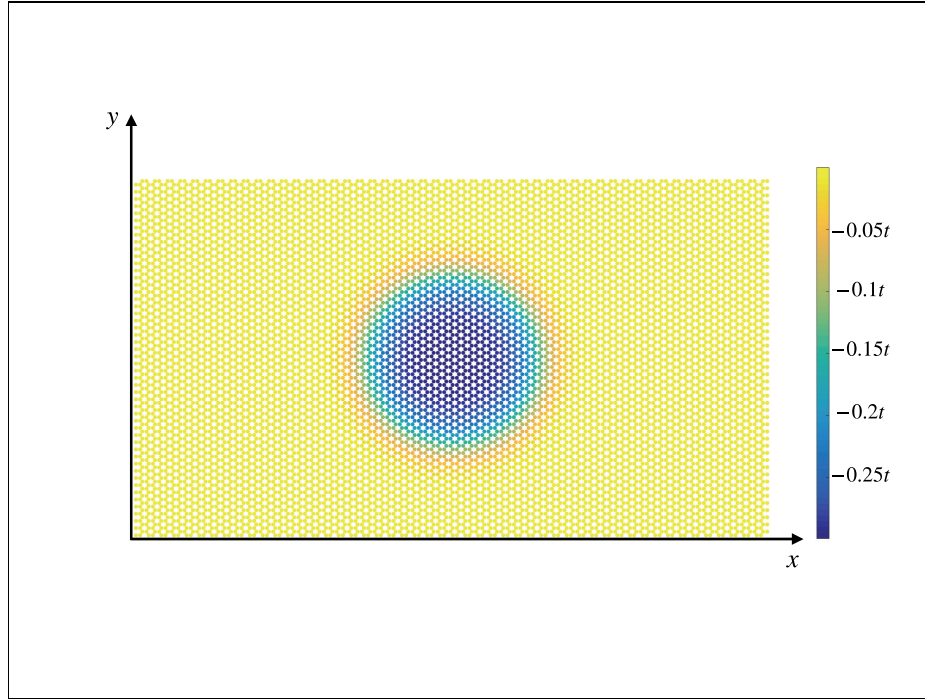
Figure 3.5. Because the system we used in our calculation consists of 22500 atoms, it is not practical to show all the atoms in one figure. Thus the figure represents the small version of the system. There is a smoothly varying sigmoid potential in the center of the system.

interaction does not decay in this case. Even for the farthest point (where $\phi = 180°$), RKKY interaction survives.

Figure 3.2 shows the enhancement in the local density of states (LDOS). We know that RKKY interaction is sensitive to density of states because higher DOS corresponds to much more state that can the magnetic moments communicate upon. Thus, if we tune Fermi level to the nearest LDOS peak, we expect even larger enhancement in RKKY.

We test the idea by slowly changing the Fermi level and we do same calculations as mentioned previously. As can be seen in figure 3.2, for Ratio=0.58, RKKY interaction relatively more enhanced compared to the other doped case. Here, Ratio means that the ratio of occupied states to unoccupied states. Therefore Ratio=0.50 corresponds to neutral case and, as the ratio increases, the Fermi level shifts upwards.
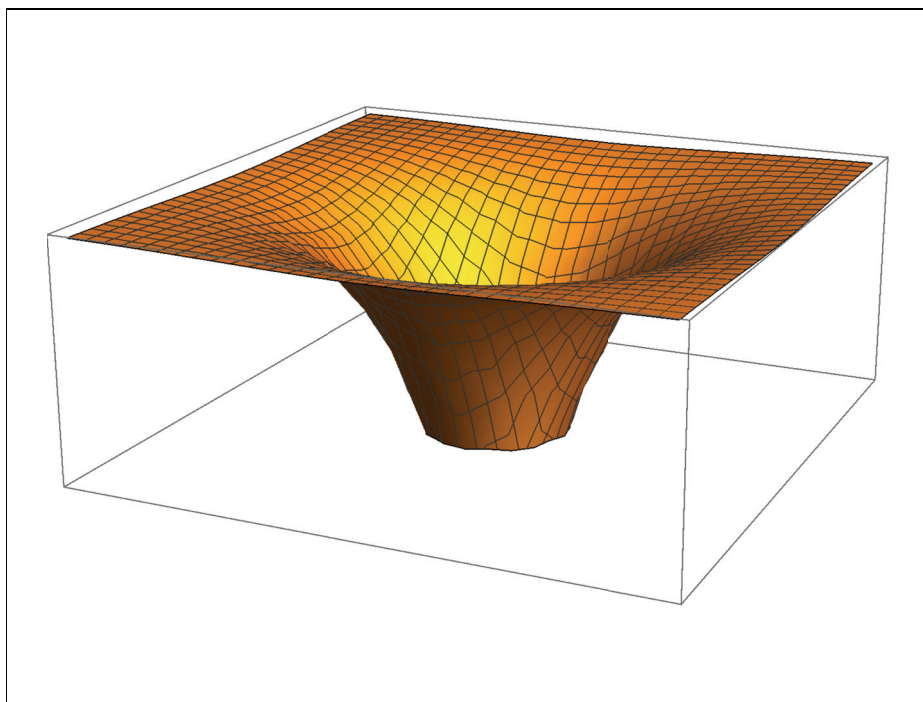
Figure 3.6. Figure shows the behaviour of sigmoid potential.
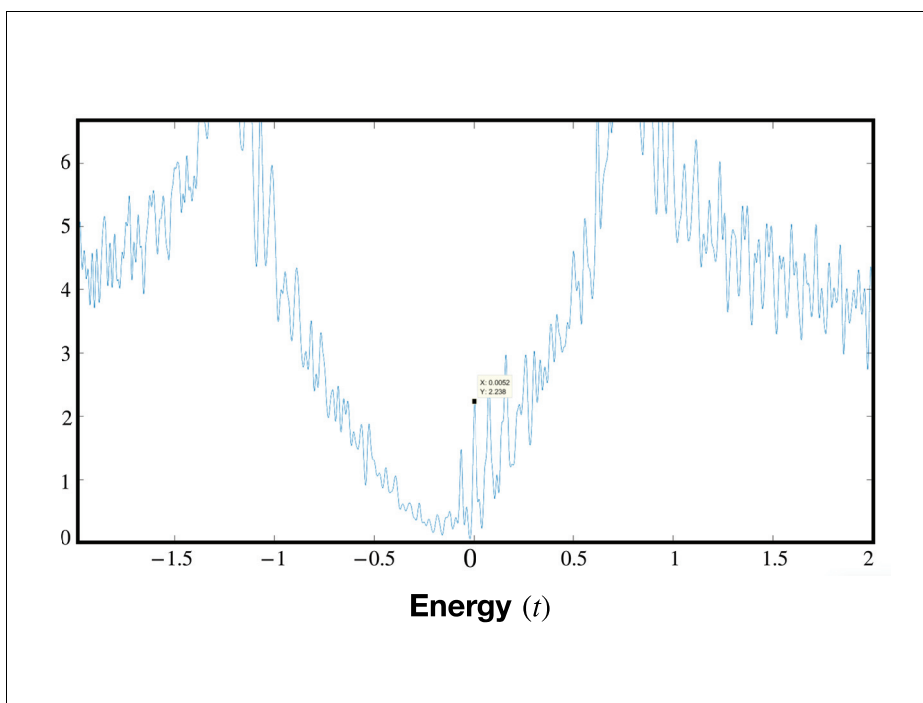
Figure 3.7. Local density of states under absence of circular potential.
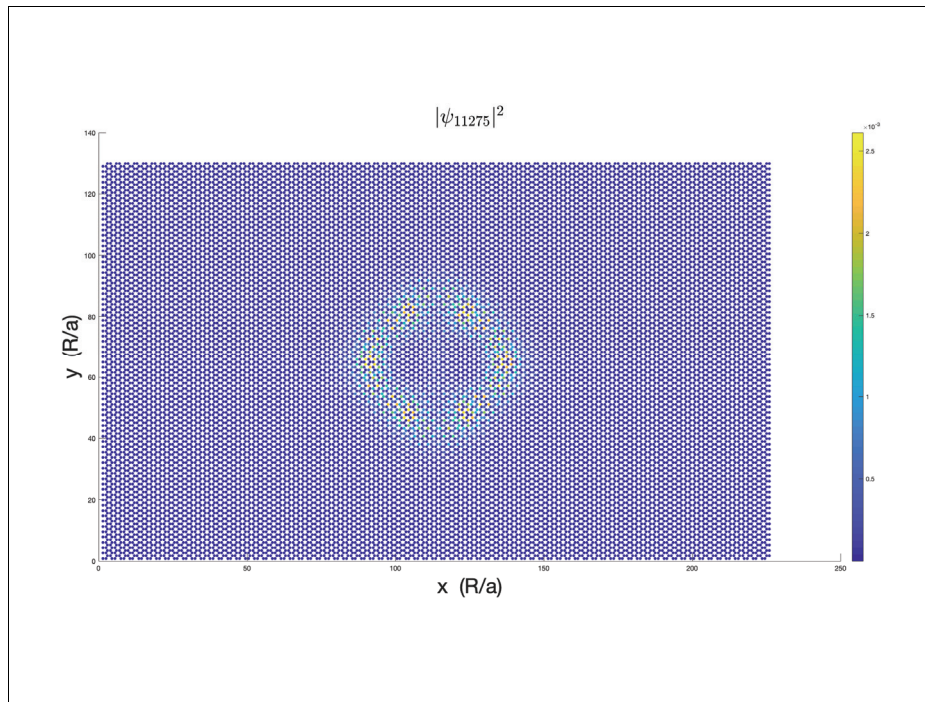
Figure 3.8. An example of confined state in a potential region as anticipated. In this case, this state 11275th state in the system. Yellow dots indicates higher probability.
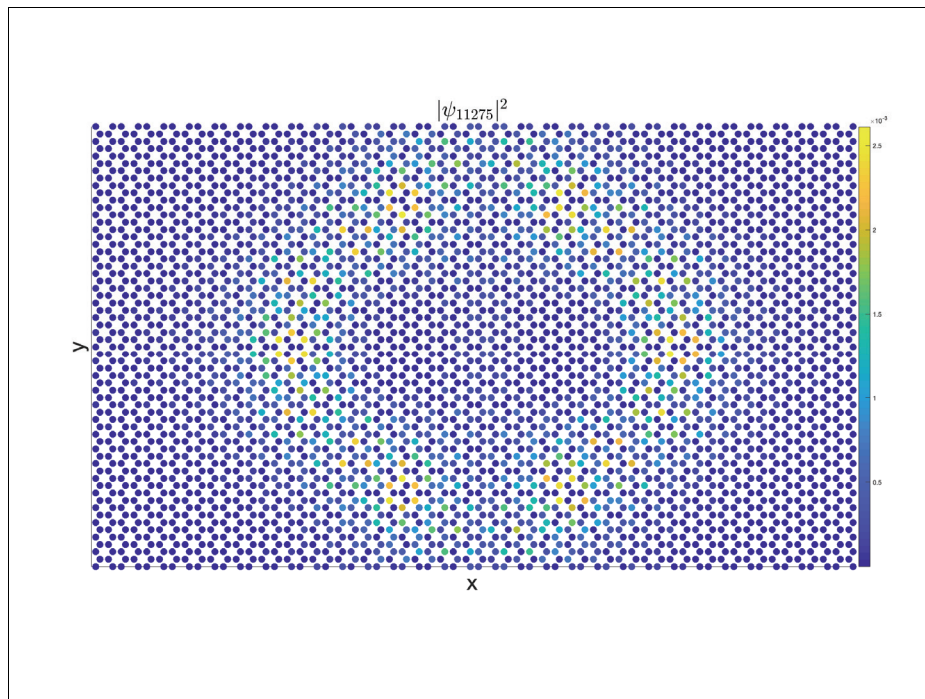
Figure 3.9. Closer look to 11275th state. It is apparent that it has confined modes in the potential region. Yellow dots indicate higher probability.
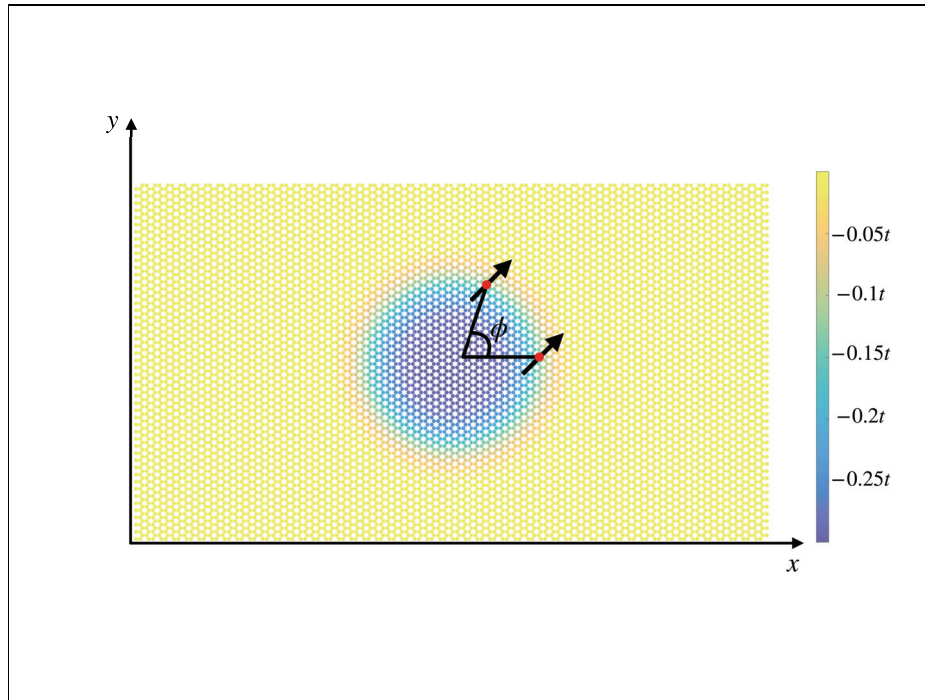
Figure 3.10. The magnetic moments are put on the half maximum of the sigmoid potential. ϕ is the angle between these moments.
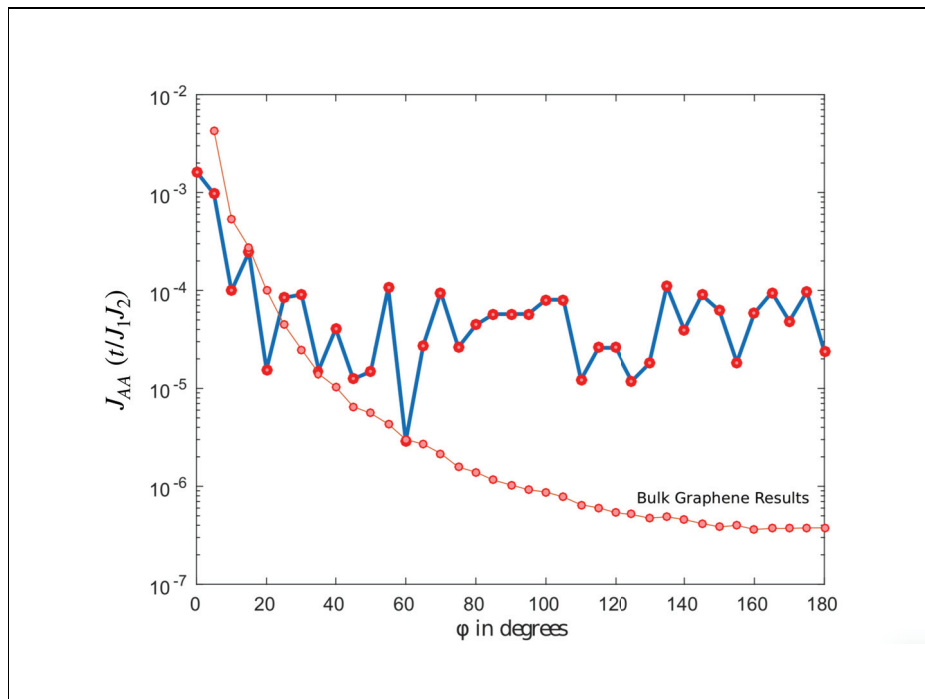
Figure 3.11. The strength of RKKY interaction as a function of the angle between the magnetic moments.
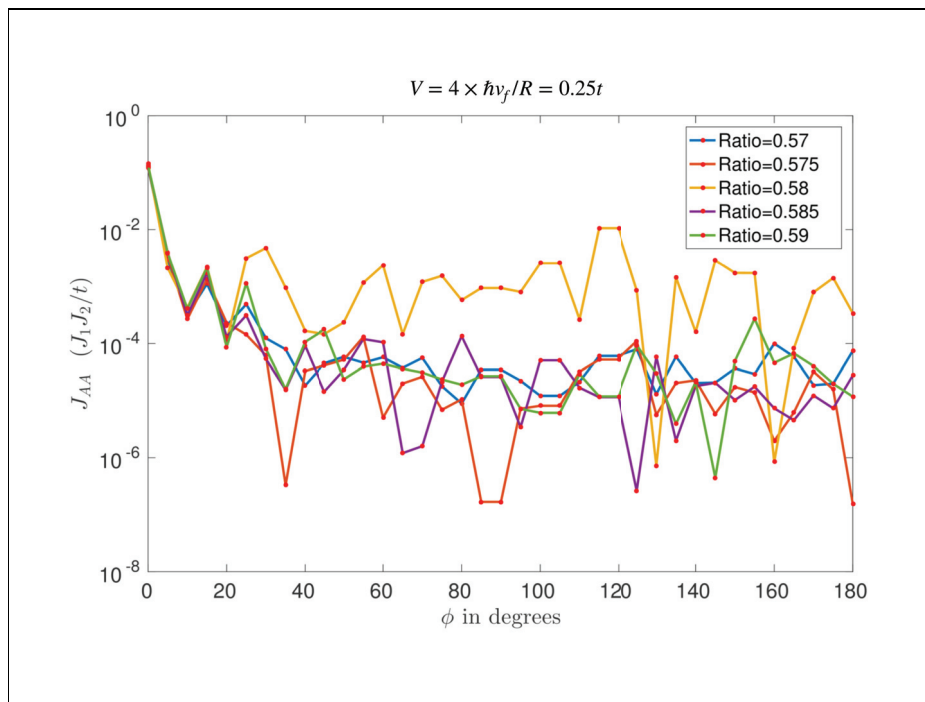
Figure 3.12. The strength of RKKY interaction for different doping level. The interaction is even more enhanced when the Fermi level matches with the energy of the first peak of the local density of states.

CHAPTER 4

RKKY INTERACTION IN GRAPHENE HEXAGONAL

FLAKE

Bulk graphene has already many unique features mentioned previously. It has also more features that can be obtained geometrically. When we cut graphene sheet into zigzag edge hexagonal lattice, there forms zero-energy states at the edges (Sun et al., 2013; Fujita et al., 1996; Nakada et al., 1996). We know that RKKY interaction is strong between states with same or close energies from the formula 1.120. Thus, we expect that the electrons between the edge of hexagonal flake interact more strongly since they share the same energy. The continuum model cannot be used in this case since there is no translational symmetry in the system. Thus, we must use tight binding approximation here. Because there are more degeneracy, electron-electron interaction is important in this case. Thus, we also include electron-electron interaction to our Hamiltonian by adding Hubbard U term. The Hamiltonian of the system can be written as

$$H = -t \sum_{<i,j>} c_j^\dagger c_i + U \sum_i n_{i\uparrow} n_{i\downarrow} + J \sum_i I_i \cdot S_i \qquad (4.1)$$

This is the Hubbard model described in detail section 2.1 about Hubbard Model. i and j are the lattice sites on the hexagonal flake and we only consider the nearest neighbor hopping. We then used mean field approximation and obtain the Hubbard Mean Field term as

$$H = -t \sum_{<i,j>\sigma} \left(c_i^\dagger c_j + h.c. \right) + U \sum_i \left(n_{i\uparrow} \langle n_{i\downarrow} \rangle + \langle n_{i\uparrow} \rangle n_{i\downarrow} - \langle n_{i\uparrow} \rangle \langle n_{i\downarrow} \rangle \right) + J \sum_i I_i \cdot S_i \quad (4.2)$$

Here, we recursively solve the Hamiltonian. After convergence is satisfied, we obtain the eigenvalues and eigenstates of the system. Finally, we could calculate the indirect exchange interaction by simply taking the enegy difference between ferromagnetic and antiferromagnetic configurations (i.e. E(FM)-E(AFM)).

In the figure above, we can see the eigenvalue index vs energy graph. The eigenvalue index simply shows that the energy of the corresponding eigenvalue after sorting them with respect to energy. In the system, we have 600 atoms. This correspond to a
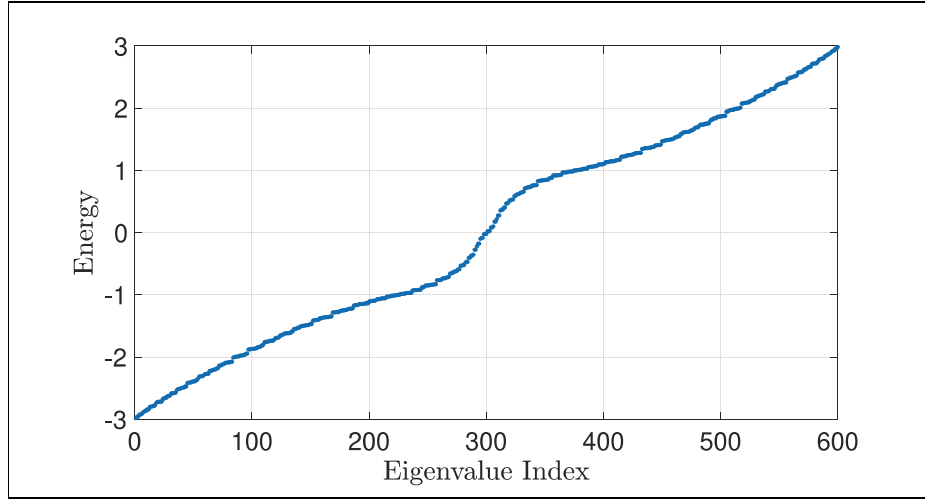
Figure 4.1. Density of states of hexagonal graphene flake with $N_s = 10$ atoms.

flake whose one edge consists of 10 atoms. We denote the number of atoms on the edge as N_s. As can be seen in the figure, there are zero energy states near eigenvalue index 300 and also states with closer energies. This zero energy states correspond to edge states.

In figure 4.2, we can see the whole system. We put one magnetic moment at the point indicated with red circle. We calculate the indirect exchange between this point and the rest of the points. The blue dots in this indirect exchange map shows the enhancement near each edge as expected. The distance between the magnetic moment we put and the edge on the opposite edge is $30a$. In bulk graphene, we know that the interaction strength decay as $1/R^3$ therefore the interaction would be insignificant at a distance $30a$ for bulk graphene.
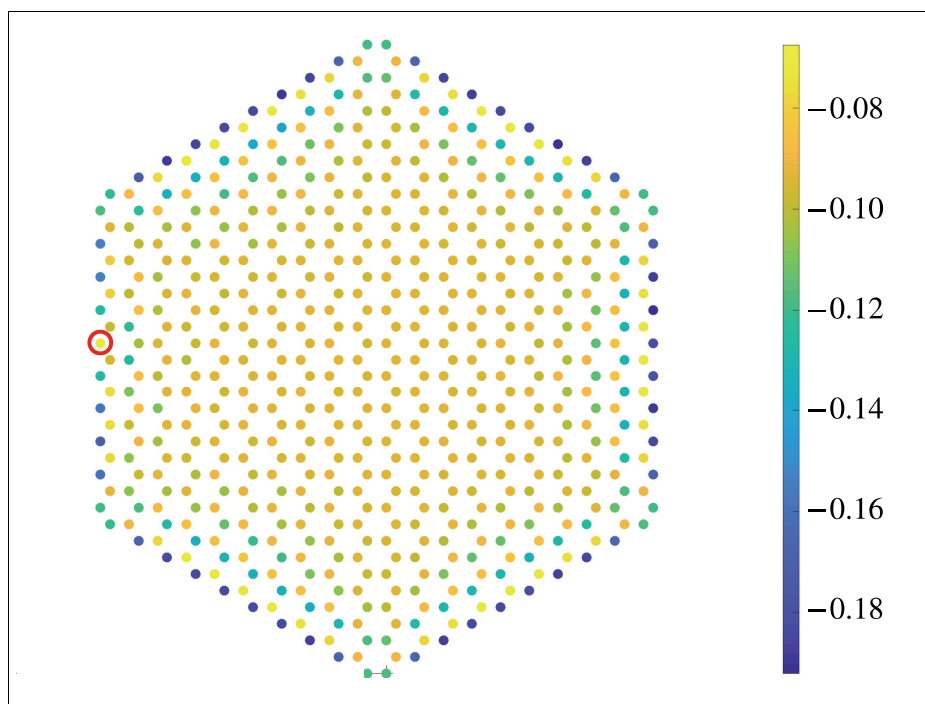
Figure 4.2. RKKY interaction map of hexagonal graphene flake with $N_s = 10$ atoms. Here, N_s represents the number of atoms on each sides.

CHAPTER 5

LONG RANGE RKKY INTERACTION IN MATERIALS WITH QUARTIC DISPERSION

As mentioned in the introduction, graphene lead the two dimensional material physics. There are many materials which have similar geometric structure with graphene. Some of these materials have their own unique character which is quartic energy dispersion. An energy dispersion is said to be quartic if it is of the form $E = \alpha(k^2 - k_c^2)^2$ where α and k_c are material dependent constants. If an energy dispersion is of the form $E = \alpha k^4$, then it is said to be pure quartic. There are many materials exhibiting quartic energy dispersion such as nitrogene, arsenene, phosphorene (Sevinçli, 2017; Kamal and Ezawa, 2015). Table 5 shows some of these materials and their respective α and k_c values. All of them are two dimensional and in hexagonal structure.

The remarkable feature of these materials is that they have van-Hove singularities in their density of states. The singularity lies next to the band-edge. Figure 5.1 shows that the form of the quartic dispersion and its corresponding density of states for two-dimenstional hexagonal lattice. There is also a discontinuity in DOS at the energy value $-\alpha k_c^4$.

In this part, we start with an Hamiltonian including second order hopping. We also add spin-spin interaction term.

$$H = -t_1 \sum_{<i,j>} (c_i^\dagger c_j + h.c.) - t_2 \sum_{<<i,j>>} (c_i^\dagger c_j + h.c.) - J \sum_{i,j} I_i \cdot S_j \qquad (5.1)$$

where c_i and $c_i^\dagger$ are annihilation and creation operators; t_1 and t_2 are first and second nearest neighbor hopping parameters, respectively. J is the coupling between

	N	P	As	Sb	Bi
α (Å^{4}eV)	1.155	2.887	3.914	5.518	8.983
k_c 1/Å	0.798	0.613	0.474	0.396	2.258

Table 5.1. Parameters for quartic dispersion for nitrogene (N), phosphorene (P), arsenene (As), antimonene (Sb) and bismuthene (Bi).
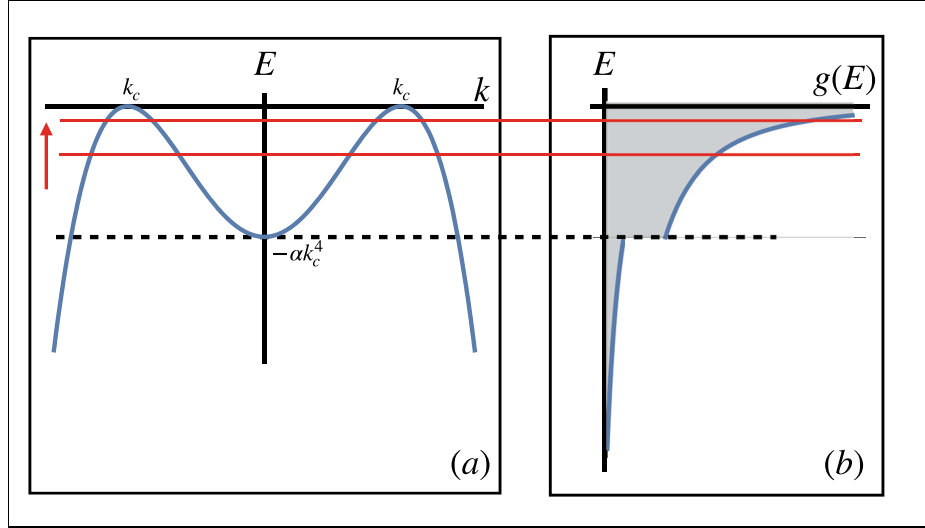
Figure 5.1. Figure (a) shows the profile of quartic dispersion. Figure (b) is the corresponding density of states for two-dimension.

localized moments I_i and conduction electrons S_j. We first focus on first and second terms (tight-binding terms) and find the effective dispersion relation. The general solution of the Hamiltonian is $E_\pm = \pm\sqrt{3 + f(k)} - t_2 f(k)$ where $f(k) = 2\cos\left(\sqrt{3}k_y a\right) + 4\cos\left(\sqrt{3}k_y a/2\right)\cos(3k_x a/2)$. Here a is the lattice constant k_x and k_y are the wavevectors of corresponding directions. Here, we are considering group-VA elements therefore there is one more extra electron per atom. This means that we are filling the upper band as well.

5.1. Quartic Dispersion

From RKKY theory, we know that the interactions between localized magnetic moments can be written as the Heisenberg type spin-spin interaction as

$$E(R) = J I_i \cdot I_j \tag{5.2}$$

where J is the exchange coupling. J can also be written in terms of spin independent susceptibility χ as

$$J = \frac{J_1 J_2 \hbar^2}{4}\chi(R) \tag{5.3}$$

Here, J_1 and J_2 are the coupling between conduction electrons and the localized

magnetic moments. χ can be written in terms of unperturbed retarded Green's function (Sherafati and Satpathy, 2011):

$$\chi(r, r') = -\frac{2}{\pi} \int_{-\infty}^{E_F} \mathrm{d}E \,\, \mathrm{Im}\{G(r, r', E)G(r', r, E)\} \tag{5.4}$$

We can write the retarded Green's function of the system as

$$G(r_1, r_2) = \sum_k \frac{\phi_k^*(r_2)\phi_k(r_1)}{\epsilon - k^4 - \mathrm{i}\delta} \tag{5.5}$$

where $\phi_k(r) = e^{\mathrm{i}k \cdot r}$. Here, we do not have to consider the interaction between two sublattices because of the system is isotropic around the gamma point in Brillouin zone. For quartic dispersion, the Green's function in the continuous spectrum becomes

$$G(r_1, r_2) = \frac{1}{(2\pi)^2} \int_{-\infty}^{\infty} \mathrm{dk_x} \int_{-\infty}^{\infty} \mathrm{dk_y} \frac{e^{\mathrm{i}k \cdot r_1} e^{-\mathrm{i}k \cdot r_2}}{\alpha(k_y^2 + k_x^2 - k_c^2)^2 - q^4 + \mathrm{i}\delta} \tag{5.6}$$

After evaluating the integral, we obtain the Green's function for $E > -\alpha k_c^4$

$$G(q, k_c, R) = -\frac{1}{8\pi\alpha k^2} \left[2K_0\left(\sqrt{q^2 - k_c^2}R\right) + \mathrm{i}\pi H_0^{(1)}\left(\sqrt{q^2 + k_c^2}R\right) \right] \tag{5.7}$$

and for $E < -\alpha k_c^4$

$$G(k, k_c, R) = \frac{\mathrm{i}}{8\alpha k^2} \left[H_0^{(1)}\left(\sqrt{k_c^2 - k^2}\, R\right) + H_0^{(1)}\left(\sqrt{k_c^2 + k^2}\, R\right) \right] \tag{5.8}$$

Here, K_0 and $H_0^{(1)}$ are modified Bessel function of second kind and Hankel function of first kind, respectively. Substituting the Green's functions into the susceptibility Equation 5.4 yields, for $E < -\alpha k^4$

$$f_1(R) = -\frac{1}{8\pi^2\alpha} \int_{-\infty}^{-\alpha k_c^4} \frac{1}{k} \left[\left(K_0(\sqrt{k^2 - k_c^2}R) - \pi N_0(\sqrt{k^2 + k_c^2}R) \right) \right. \tag{5.9}$$

$$\left. \times \left(\pi J_0(\sqrt{k^2 + k_c^2}R) \right) \right] \, \mathrm{d}k$$

and for $E > -\alpha k^4$

$$f_2(R) = \frac{1}{8\alpha} \int_{-\alpha k_c^4}^{E_f} \frac{1}{k} \left[\left(J_0(\sqrt{k_c^2 - k^2}R) + J_0(\sqrt{k_c^2 + k^2}R) \right) \right. \tag{5.10}$$

$$\left. \times \left(N_0(\sqrt{k_c^2 + k^2}R) - N_0(\sqrt{k_c^2 - k^2}R) \right) \right] \, \mathrm{d}k$$

Since there are two regions $E < -\alpha k^4$ and $E > -\alpha k^4$, the susceptibility near band-edge becomes the sum of these two susceptibility functions

$$\chi(E, R) = f_1(R) + f_2(R) \tag{5.11}$$

The first term gives constant contribution since $-\alpha k_c^4$ is constant. Here, it is difficult to analytically calculate the susceptibility function, therefore we calculate it numerically for each R. We first fix α and k_c values and calculate the susceptibility as a function of R for different Fermi levels E_f. We start with a Fermi level in upper part of the Mexican hat and shift it near band edge as close as possible to catch the singularity in the density of states. The red lines in figure 5.1 shows the Fermi level and the red arrow indicates the direction of the shift.
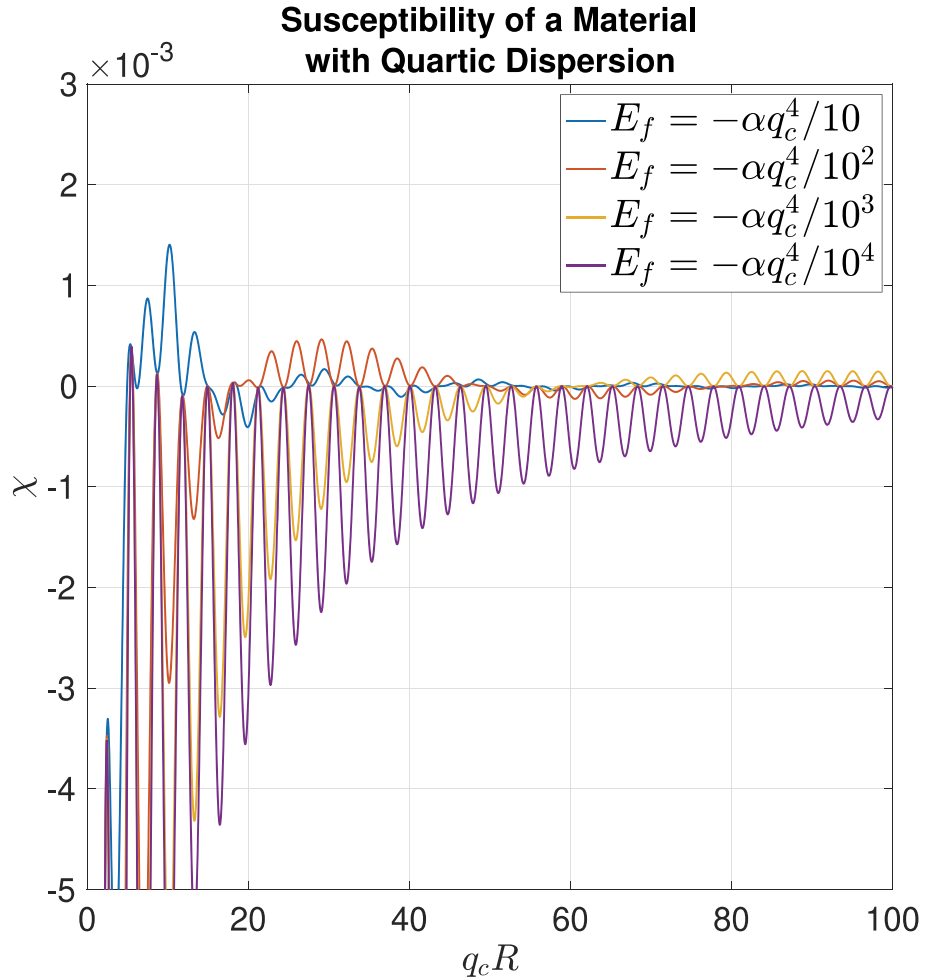

Figure 5.2. Susceptibility as a function of R

As can be seen in the figure 5.2, the Fermi level gets smaller (i.e. closer to the

band-edge) the interaction strength is greatly enhanced. There is a competition between k_c and k_f. The small oscillations are on the order of $1/k_c$ and the large oscillations which gives fluctuations between ferromagnetic and anti-ferromagnetic behavior are on the order of $1/k_f$. For an arbitrarily small Fermi levels the indirect exchange interaction becomes long range.

5.2. Pure Quartic Dispersion

In this section, we calculated the indirect exchange interaction both analytically and numerically. For analytic calculation, we used retarded Green's function. For numerical calculations we used tight-binding model with exact diagonalization, perturbation and the integral expansion which introduced in the Methods section.

5.2.1. Analytical Calculation of Susceptibility

Pure quartic dispersion indicates when $k_c = 0$ therefore $E = \alpha k_c^4$. We already found the susceptibility as a function of R, k and k_c in the previous chapter. We can now either calculate the Green's function for our pure quartic dispersion or we can simply take $k_c \to 0$. The results will be same. The explicit calculations can be found in the appendix. Hence, the Green's function for pure quartic dispersion is

$$G(k, R) = -\frac{1}{8\pi\alpha k^2} \left(2K_0(kR) + i\pi H_0^{(1)}(kR) \right) \tag{5.12}$$

and the corresponding susceptibility becomes

$$\chi(k, R) = -\frac{1}{8\pi^2\alpha} \int_{k_f}^{\infty} \frac{1}{k} \left[(K_0(kR) - \pi N_0(kR)) \pi J_0(kR) \right] \, \mathrm{d}k \tag{5.13}$$

Here, the susceptibility function χ is only function of kR which we can choose as a dimensionless parameter and plot the graph accordingly.

In the pure quartic case, the RKKY interaction becomes long range and the range of the interaction depends on Fermi momentum k_f. As seen in figure 5.3, the x-axis is $k_f R$ which means that for small k_f values, the axis stretch and we obtain slowly decaying/long range RKKY interaction. The essential point is that k_f can be chosen arbitrarily small. Experimentally, this corresponds to dilute doping which can easily be realized.
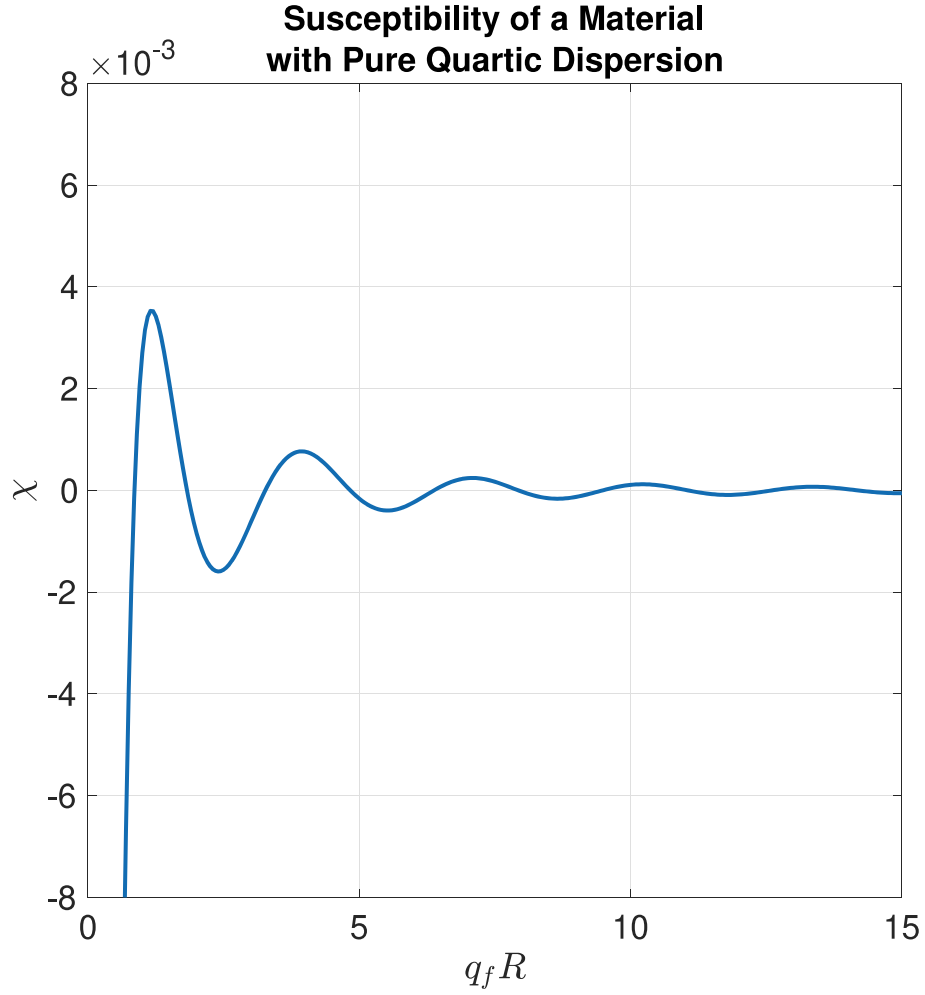
Figure 5.3. Figure shows the behavior of the susceptibility function of pure quartic dispersion.

5.2.2. Tight-Binding Calculations of RKKY Interaction

We start with tight-binding Hamiltonian including second nearest neighbor hopping.

$$H = -t_1 \sum_{<i,j>} c_i^\dagger c_j - t_2 \sum_{<<i,j>>} c_i^\dagger c_j - J \sum_i I_i \cdot S_j \qquad (5.14)$$

where t_1 and t_2 are the first and second nearest neighbor hopping constants. I_i and S_j are the spin of the localized magnetic moment and the spin of the conduction electrons, respectively. Pure quartic dispersion is a special case and it occurs when $t_2/t_1 = 1/6$. We calculated for 22500 carbon atoms and applied periodic boundary conditions. We first found the eigenvalues and eigenfunctions by only considering tight-binding part. Figure

5.4 shows the number of states with their corresponding energies. (a) shows the whole spectrum and (b) is only a small potion lying near the band-edge. On band-edge, there are more states compared to rest of the system. There cannot be a singularity in our system since we are dealing with a finite system. However, the higher amount of states at the band-edge mimics this singularity.
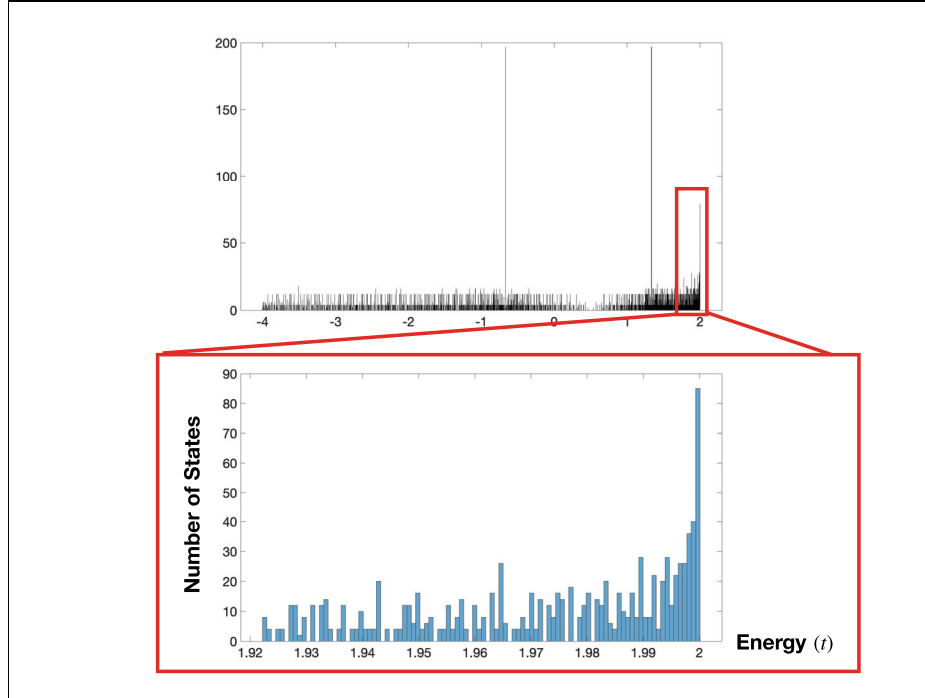
Figure 5.4. Figure shows energies and their corresponding number of states.

We treat the spin-spin interaction term in the Hamiltonian and calculate the RKKY interaction by using the following equation

$$J = J_1 J_2 \sum_{\substack{k,k' \\ i \neq j}} \frac{\Psi_k(R_i)\Psi_{k'}^*(R_i)\Psi_{k'}(R_j)\Psi_k^*(R_j)}{\epsilon_k - \epsilon_{k'}} \, n_k(1 - n_{k'}) \tag{5.15}$$

We tune the Fermi level as it lies on the "singularity" and calculate the interaction. We also used exact diagonalization and integral expansion which are covered in section Methods in detail.

In the figures above blue lines (rkky), red lines (exact diagonalization) and yellow line (analytic) represents the perturbative calculation, exact diagonalization and integral expansion, respectively. Blue and yellow lines matches pretty accurately. The exact diagonalization results agree with the others for small r values however there are deviations
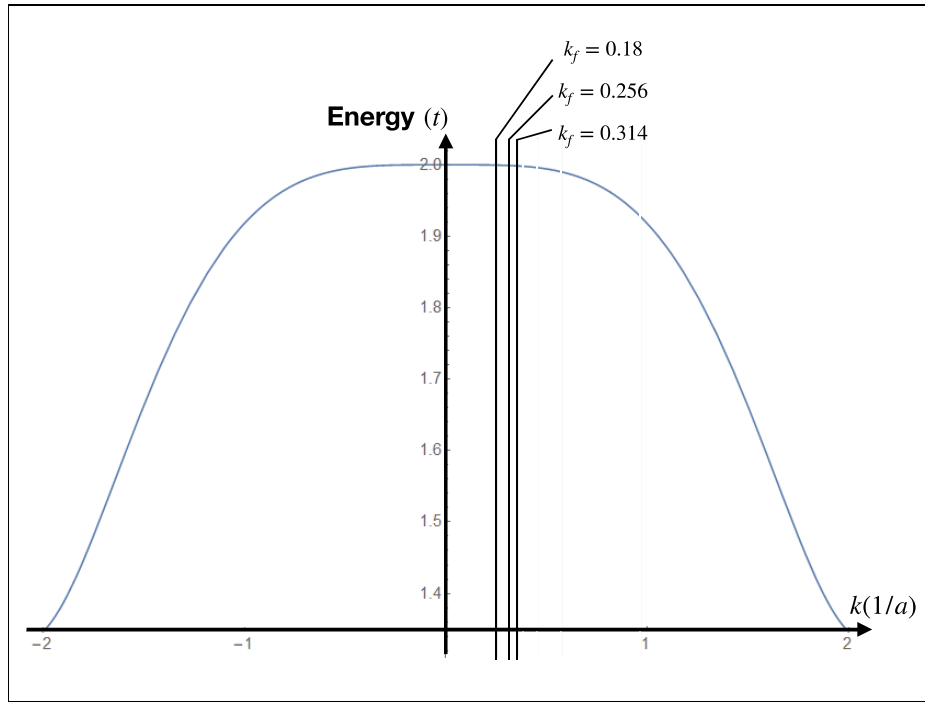
Figure 5.5. Figure shows the position of the Fermi wavelengths $k_f = 0.18$, $k_f = 0.256$ and $k_f = 0.314$ on pure quartic dispersion graph.

for large r. This is because the finite size effects because when we tune Fermi level near band-edge, the Fermi wavelength becomes comparable with the system size. Hence, it is more convenient to solve the problem analytically using retarded Green's function to avoid these finite size effects.
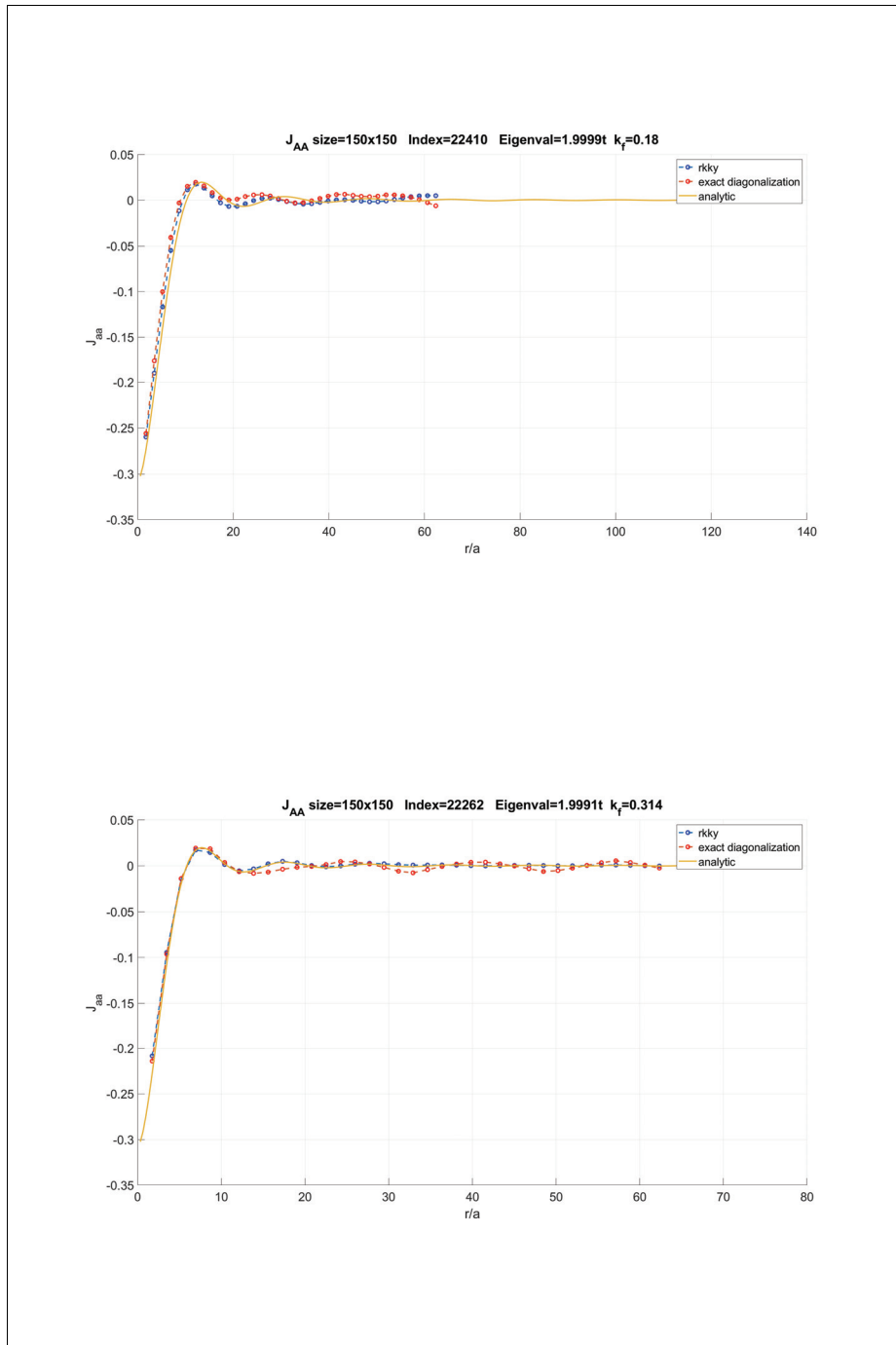
Figure 5.6. Figure shows the strength of RKKY interaction with respect to distance between magnetic moments r with comparison of different numerical methods for $k_f = 0.314\ (1/a)$

CHAPTER 6

CONCLUSIONS

There are three part in the thesis. In the first part, we calculated RKKY interaction for graphene sheet under applied circular potential. We choose smoothly varying potential to mimic a realistic external potential. We located two magnetic moments on the edge of the potential well and calculated RKKY interaction as a function of the angle between them while changing the position of a magnetic moment along the edge. We found that the interaction is enhanced due to quasi bound states form in the circular potential and it does not decay with $1/R^3$ as in bulk graphene. Here, R is the distance between the magnetic moments. We also tuned to the Fermi level so that it matches with the local density of states resonance. We found that the interaction strength is enhanced more when the Fermi level is tuned to the quasi-bound state energy.

In the second part, we calculated RKKY interaction for zigzag edged graphene nanoflakes. It is known that zigzag edged nanoflakes have zero-edge band states. These states are localized at the edge of the flake therefore they have higher density of states near edges. It is also known that RKKY interaction is enhanced for the places with higher density of states. We calculated that RKKY interaction is enhanced due to these zero-energy band states. The RKKY interaction still remain for large distances that we could not achieve for bulk graphene. The enhanced spin-spin correlation between these edge states is a good candidate for spintronic applications.

In the third part, we investigated the behaviour of RKKY interaction for quartic and pure quartic materials. We used both numerical and analytic techniques to cross-check. We first calculated RKKY interaction perturbatively and with exact diagonalization in tight-binding approximation. We numerically expand the perturbation expression as well. We also found the Green's function in the effective mass approximation and calculate the RKKY interaction analytically in the bulk limit. We found that for quartic materials the interaction is enhanced due to the van-Hove singularity near band-edge. Unlike the ordinary two dimensional metals where RKKY interaction decays as R^3, quartic materials exhibit long range behavior depending on the material dependent constant k_c. For materials with pure quartic dispersion, the interaction becomes long range for arbitrarily chosen small Fermi level.

REFERENCES

Allain, P. E. and J. N. Fuchs (2011, October). Klein tunneling in graphene: optics with massless electrons. *The European Physical Journal B 83*(3), 301–317.

Ashcroft, N. and N. Mermin (1976). *Solid State Physics*. HRW international editions. Holt, Rinehart and Winston.

Bena, C. and G. Montambaux (2009, sep). Remarks on the tight-binding model of graphene. *New Journal of Physics 11*(9), 095003.

Black-Schaffer, A. M. (2010a, August). Importance of electron-electron interactions in the RKKY coupling in graphene. *Physical Review B 82*(7).

Black-Schaffer, A. M. (2010b, May). Rkky coupling in graphene. *Phys. Rev. B 81*, 205416.

Castro Neto, A. H., F. Guinea, N. M. R. Peres, K. S. Novoselov, and A. K. Geim (2009, Jan). The electronic properties of graphene. *Rev. Mod. Phys. 81*, 109–162.

Choi, W., I. Lahiri, R. Seelaboyina, and Y. S. Kang (2010, February). Synthesis of graphene and its applications: A review. *Critical Reviews in Solid State and Materials Sciences 35*(1), 52–71.

Deaven, D. M., D. S. Rokhsar, and M. Johnson (1991, Sep). Simple theory of exchange coupling in transition-metal magnetic multilayers. *Phys. Rev. B 44*, 5977–5980.

Fujita, M., K. Wakabayashi, K. Nakada, and K. Kusakabe (1996, July). Peculiar localized state at zigzag graphite edge. *Journal of the Physical Society of Japan 65*(7), 1920–1923.

Geim, A. K. and K. S. Novoselov (2007, mar). The rise of graphene. *Nature Materials 6*, 183.

Greiner, W. and D. Bromley (2000). *Relativistic Quantum Mechanics. Wave Equations*. Springer.

Greiner, W., B. Müller, and J. Rafelski (1985). The klein paradox. In *Quantum Electrodynamics of Strong Fields*, pp. 112–121. Springer Berlin Heidelberg.

Guclu, A., P. Potasz, and M. Korkusinski (2014). *Graphene Quantum Dots*. Springer.

Kamal, C. and M. Ezawa (2015, Feb). Arsenene: Two-dimensional buckled and puckered honeycomb arsenic systems. *Phys. Rev. B 91*, 085423.

Kasuya, T. (1956, 07). A Theory of Metallic Ferro- and Antiferromagnetism on Zener's Model. *Progress of Theoretical Physics 16*(1), 45–57.

Katsnelson, M. I., K. S. Novoselov, and A. K. Geim (2006a, August). Chiral tunnelling and the klein paradox in graphene. *Nature Physics 2*(9), 620–625.

Katsnelson, M. I., K. S. Novoselov, and A. K. Geim (2006b). Chiral tunnelling and the Klein paradox inÂ graphene. *Nature Physics 2*(9), 620–625.

Kittel, C. (1963). *Quantum Theory of Solids*. New York: Wiley.

Kittel, C. (2004). *Introduction to Solid State Physics* (8 ed.). Wiley.

Kogan, E. (2011, Sep). Rkky interaction in graphene. *Phys. Rev. B 84*, 115119.

Marder, M. (2010). *Condensed Matter Physics*. Wiley.

Nakada, K., M. Fujita, G. Dresselhaus, and M. S. Dresselhaus (1996, Dec). Edge state in graphene ribbons: Nanometer size effect and edge shape dependence. *Phys. Rev. B 54*, 17954–17961.

Nolting, W. and A. Ramakanth (2009). *Quantum Theory of Magnetism*. Springer Berlin Heidelberg.

Novoselov, K. S., A. K. Geim, S. V. Morozov, D. Jiang, Y. Zhang, S. V. Dubonos, I. V. Grigorieva, and A. A. Firsov (2004). Electric field effect in atomically thin carbon films. *Science 306*(5696), 666–669.

Novoselov, falko, V. I., L. Colombo, P. R. Gellert, M. G. Schwab, and K. Kim (2012,

oct). A roadmap for graphene. *Nature 490*, 192.

Power, S. and M. Ferreira (2013, January). Indirect exchange and ruderman–kittel–kasuya–yosida (RKKY) interactions in magnetically-doped graphene. *Crystals 3*(1), 49–78.

Reich, S., J. Maultzsch, C. Thomsen, and P. Ordejón (2002, July). Tight-binding description of graphene. *Physical Review B 66*(3).

Ruderman, M. A. and C. Kittel (1954, Oct). Indirect exchange coupling of nuclear magnetic moments by conduction electrons. *Phys. Rev. 96*, 99–102.

Saito, R., G. Dresselhaus, and M. S. Dresselhaus (1998, July). *Physical Properties of Carbon Nanotubes*. Published by Imperial College Press and Distributed by World Scientific Publishing CO.

Saremi, S. (2007, Nov). Rkky in half-filled bipartite lattices: Graphene as an example. *Phys. Rev. B 76*, 184430.

Sevinçli, H. (2017). Quartic Dispersion, Strong Singularity, Magnetic Instability, and Unique Thermoelectric Properties in Two-Dimensional Hexagonal Lattices of Group-VA Elements. *Nano Letters 17*(4), 2589–2595.

Sherafati, M. and S. Satpathy (2011, Apr). Rkky interaction in graphene from the lattice green's function. *Phys. Rev. B 83*, 165425.

Shytov, A. V., M. I. Katsnelson, and L. S. Levitov (2007, Dec). Atomic collapse and quasi–rydberg states in graphene. *Phys. Rev. Lett. 99*, 246802.

Sun, J. H., F. M. Hu, H. K. Tang, W. Guo, and H. Q. Lin (2013, May). Indirect exchange of magnetic impurities in zigzag graphene ribbon. *Journal of Applied Physics 113*(17), 17B515.

Wallace, P. R. (1947, May). The band theory of graphite. *Phys. Rev. 71*, 622–634.

Wang, Y., D. Wong, A. V. Shytov, V. W. Brar, S. Choi, Q. Wu, H.-Z. Tsai, W. Regan, A. Zettl, R. K. Kawakami, S. G. Louie, L. S. Levitov, and M. F. Crommie (2013).

Observing atomic collapse resonances in artificial nuclei on graphene. *Science 340*(6133), 734–737.

Yosida, K. (1957, Jun). Magnetic properties of cu-mn alloys. *Phys. Rev. 106*, 893–898.

Young, A. F. and P. Kim (2009, February). Quantum interference and klein tunnelling in graphene heterojunctions. *Nature Physics 5*(3), 222–226.

Zarenia, M., A. Chaves, G. A. Farias, and F. M. Peeters (2011, Dec). Energy levels of triangular and hexagonal graphene quantum dots: A comparative study between the tight-binding and dirac equation approach. *Phys. Rev. B 84*, 245403.

Zhao, Y., J. Wyrick, F. D. Natterer, J. F. Rodriguez-Nieva, C. Lewandowski, K. Watanabe, T. Taniguchi, L. S. Levitov, N. B. Zhitenev, and J. A. Stroscio (2015). Creating and probing electron whispering-gallery modes in graphene. *Science 348*(6235), 672–675.

APPENDIX A

EXPLICIT ANALYTICAL CALCULATION OF RKKY INTERACTION FOR MATERIALS WITH QUARTIC DISPERSION

In this chapter, we explicitly show the calculation of Green's function for quartic dispersion ($E = -\alpha(k^2 - k_c^2)^2$) and pure quartic dispersion ($E = -\alpha k^4$). From the Green's function, we also compute the susceptibility χ as a function of R.

A.1. Pure Quartic Calculations

We can make an eigenstate expansion using the retarded Green's function as follows:

$$G(r_1, r_2) = \sum_k \frac{\phi_k^*(r_2)\phi_k(r_1)}{\epsilon + q^4 + i\delta} \tag{A.1}$$

Here, ϵ_k's are the eigenvalues of the Hamiltonian i.e.

$$H\phi_k = \epsilon_k \phi_k \tag{A.2}$$

and the corresponding eigenstates are

$$\phi_k(r) = \begin{pmatrix} 1 \\ e^{i\theta} \end{pmatrix} e^{ik \cdot r} \tag{A.3}$$

Because our system is bipartite, the eigenstate has extra pseudospin term. However, we are dealing with the interaction between same sites so we take $\phi_k(r) = e^{ik \cdot r}$. Since we have a quartic dispersion, $\epsilon = -\alpha k^4$ with $\alpha > 0$. Then, the Green's function becomes in the continuous spectrum

$$G(r_1, r_2) = \frac{1}{(2\pi)^2} \int_{-\infty}^{\infty} \mathrm{dk_x} \int_{-\infty}^{\infty} \mathrm{dk_y} \frac{e^{ik \cdot r_1} e^{-ik \cdot r_2}}{\alpha(k_x^2 + k_y^2)^2 - q^4 + i\delta} \tag{A.4}$$

We can choose $R \equiv r_1 - r_2$ along x-direction without loss of generality and also redefine $q^4 = q^4 \alpha$. The Green's function then becomes
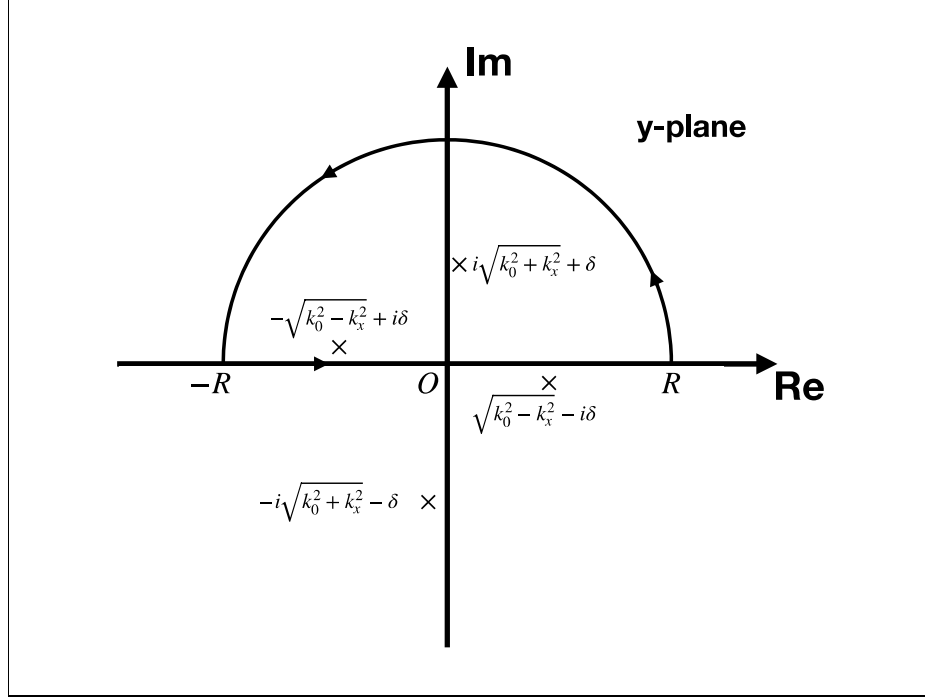

Figure A.1. The contour and the simple poles of the integral when $|q| > |k_x|$.

$$G(r_1, r_2) = \frac{1}{(2\pi)^2 \alpha} \int_{-\infty}^{\infty} dk_x \, e^{ik_x R} \underbrace{\int_{-\infty}^{\infty} \frac{dk_y}{(k_x^2 + k_y^2)^2 - q^4 + i\delta}}_{I(k_x)} \qquad (A.5)$$

To evaluate the integral $I(k_x)$, one must find the poles. $I(k_x)$ has six different simple poles. For $|q| > |k_x|$,

$$k_{y,(1,2)} = \sqrt{-q^2 - k_x^2 + i\delta} = \pm i\sqrt{q^2 + k_x^2 - i\delta} = \pm i\sqrt{q^2 + k_x^2} \pm \delta \qquad (A.6)$$

$$k_{y,(3,4)} = \sqrt{q^2 - k_x^2 - i\delta} = \pm\sqrt{q^2 - k_x^2} \pm i\delta \qquad (A.7)$$

For the case $|q| < |k_x|$, the poles are:

$$k_{y,(1,2)} = \sqrt{-q^2 - k_x^2 + i\delta} = \pm i\sqrt{q^2 + k_x^2 - i\delta} = \pm i\sqrt{q^2 + k_x^2} \pm \delta \qquad (A.8)$$

$$k_{y,(5,6)} = \sqrt{q^2 - k_x^2 - i\delta} = \pm i\sqrt{k_x^2 - q^2} \pm \delta \qquad (A.9)$$

63
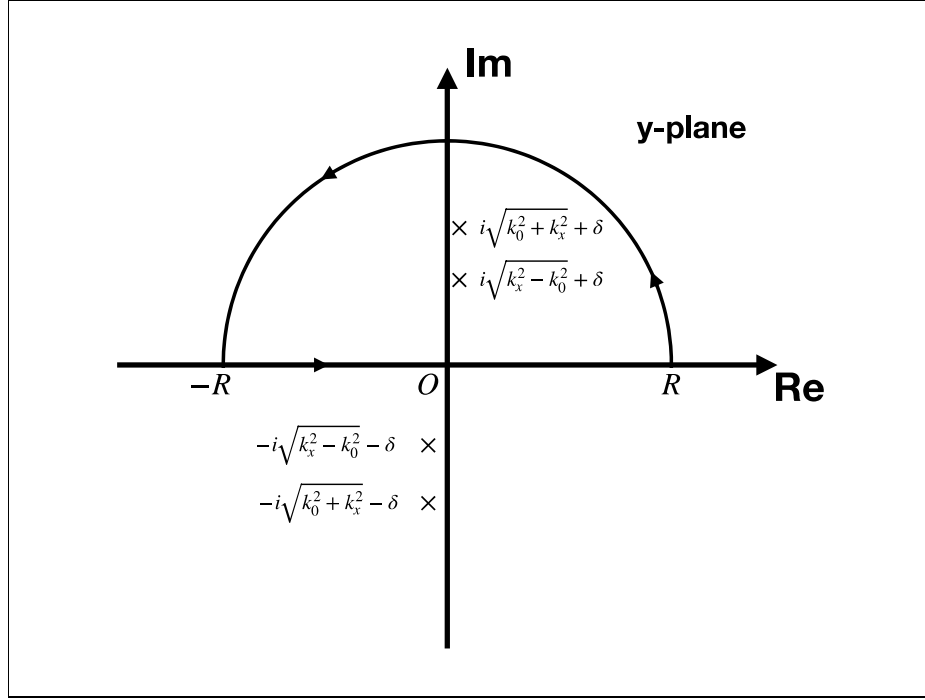
Figure A.2. The contour and the simple poles of the integral when $|q| < |k_x|$.

Lemma: Let f have a simple pole at z_0, and let g be holomorphic at z_0. Then,

$$\text{Res}_{z_0}(fg) = g(z_0)\,\text{Res}_{z_0} f \tag{A.10}$$

Since we have more than one pole, we need to use the lemma above and evaluate the integral for the two cases, separately.

For $|k_x| < |q|$,

$$
\begin{aligned}
I(k_x) &= 2\pi\mathrm{i}\left[g\left(i\sqrt{q^2+k_x^2}\right)\text{Res}_{i\sqrt{q^2+k_x^2}}(f)\right. \tag{A.11}\\
&+ \left. g\left(-\sqrt{q^2-k_x^2}\right)\text{Res}_{-\sqrt{q^2-k_x^2}}(f)\right]\\
I(k_x) &= 2\pi\mathrm{i}\left(\frac{\mathrm{i}}{4q^2\sqrt{q^2+k_x^2}} - \frac{1}{4q^2\sqrt{q^2-k_x^2}}\right) \tag{A.12}\\
&= -\frac{\pi}{2q^2\sqrt{q^2+k_x^2}} - \frac{\pi\mathrm{i}}{2q^2\sqrt{q^2-k_x^2}}
\end{aligned}
$$

For $|k_x| > |q|$,

$$I(k_x) = 2\pi\mathrm{i} \left[g\left(i\sqrt{q^2 + k_x^2}\right) \mathrm{Res}_{i\sqrt{q^2+k_x^2}}(f) \right.$$

$$\left. + \ g\left(\mathrm{i}\sqrt{k_x^2 - q^2}\right) \mathrm{Res}_{\mathrm{i}\sqrt{k_x^2-q^2}}(f)\right] \qquad \text{(A.13)}$$

$$I(k_x) = 2\pi\mathrm{i} \left(\frac{\mathrm{i}}{4q^2\sqrt{q^2 + k_x^2}} - \frac{\mathrm{i}}{4k_x^2\sqrt{k_x^2 - q^2}} \right) \qquad \text{(A.14)}$$

$$= \frac{\pi}{2q^2\sqrt{k_x^2 - q^2}} - \frac{\pi}{2q^2\sqrt{q^2 + k_x^2}} \qquad \text{(A.15)}$$

Hence, the Green's function becomes

$$G(r_1, r_2) = \frac{1}{(2\pi)^2\alpha} \left(\int_{|q|<|k_x|} \mathrm{dk_x} + \int_{|k_x|>|q|} \mathrm{dk_x} \right) e^{\mathrm{i}k_x R} I(k_x) \qquad \text{(A.16)}$$

We can explicitly write as the following:

$$G(q, R) = \frac{1}{(2\pi)^2\alpha} \left[\int_{-q}^{q} - \left(\frac{\pi}{2q^2\sqrt{q^2 + k_x^2}} + \frac{\pi\mathrm{i}}{2q^2\sqrt{q^2 - k_x^2}} \right) e^{\mathrm{i}k_x R} \,\mathrm{dk_x} \right. \qquad \text{(A.17)}$$

$$+ \int_{q}^{\infty} \left(\frac{\pi}{2q^2\sqrt{k_x^2 - q^2}} - \frac{\pi}{2q^2\sqrt{q^2 + k_x^2}} \,\mathrm{dk_x} \right) e^{\mathrm{i}k_x R} \,\mathrm{dk_x}$$

$$\left. + \int_{-\infty}^{-q} \left(\frac{\pi}{2q^2\sqrt{k_x^2 - q^2}} - \frac{\pi}{2q^2\sqrt{q^2 + k_x^2}} \,\mathrm{dk_x} \right) e^{\mathrm{i}k_x R} \,\mathrm{dk_x} \right]$$

The integrals can be rearranged in the form:

$$G(q, R) = -\frac{1}{(2\pi)^2\alpha} \left[\int_{-\infty}^{\infty} \frac{\pi \,\mathrm{dk_x}}{2q^2\sqrt{q^2 + k_x^2}} e^{\mathrm{i}k_x R} + \int_{-q}^{q} \frac{\pi\mathrm{i} \,\mathrm{dk_x}}{2q^2\sqrt{q^2 - k_x^2}} e^{\mathrm{i}k_x R} \right. \qquad \text{(A.18)}$$

$$\left. - \int_{q}^{\infty} \frac{\pi}{2q^2 \underbrace{\sqrt{k_x^2 - q^2}}_{=\mathrm{i}\sqrt{q^2-k_x^2}}} e^{\mathrm{i}k_x R} \,\mathrm{dk_x} - \int_{-\infty}^{-q} \frac{\pi}{2q^2 \underbrace{\sqrt{k_x^2 - q^2}}_{=\mathrm{i}\sqrt{q^2-k_x^2}}} e^{\mathrm{i}k_x R} \,\mathrm{dk_x} \right]$$

Finally, we obtain very compact form as

$$G(q, R) = -\frac{1}{8\pi\alpha q^2} \left[\int_{-\infty}^{\infty} \frac{e^{\mathrm{i}k_x R}}{\sqrt{q^2 + k_x^2}} \,\mathrm{dk_x} + \mathrm{i} \int_{-\infty}^{\infty} \frac{e^{\mathrm{i}k_x R}}{\sqrt{q^2 - k_x^2}} \,\mathrm{dk_x} \right] \qquad \text{(A.19)}$$

After evaluating the integrals, we obtain

$$G(q, R) = -\frac{1}{8\pi\alpha q^2}\left(2K_0(qR) + i\pi H_0^{(1)}(qR)\right) \tag{A.20}$$

The result is found as the linear combination of the modified Bessel function of second kind and Hankel function of first kind.

A.2. Quartic Calculations

We can make an eigenstate expansion using the retarded Green's function as follows:

$$G(r_1, r_2) = \sum_k \frac{\phi_k^*(r_2)\phi_k(r_1)}{\epsilon + q^4 + i\delta} \tag{A.21}$$

Here, ϵ_k's are the eigenvalues of the Hamiltonian i.e.

$$H\phi_k = \epsilon_k\phi_k \tag{A.22}$$

and the corresponding eigenstates are

$$\phi_k(r) = \begin{pmatrix} 1 \\ e^{i\theta} \end{pmatrix} e^{ik\cdot r} \tag{A.23}$$

Because our system is bipartite, the eigenstate has extra pseudospin term. However, we are dealing with the interaction between same sites so we take $\phi_k(r) = e^{ik\cdot r}$. Since we have a quartic dispersion, $\epsilon = -\alpha k^4$ with $\alpha > 0$. Then, the Green's function becomes in the continuous spectrum

$$G(r_1, r_2) = \frac{1}{(2\pi)^2}\int_{-\infty}^{\infty}dk_x\int_{-\infty}^{\infty}dk_y\frac{e^{ik\cdot r_1}e^{-ik\cdot r_2}}{\alpha(k_y^2 + k_x^2 - k_c^2)^2 - q^4 + i\delta} \tag{A.24}$$

We can choose $R \equiv r_1 - r_2$ along x-direction without loss of generality and also redefine $q^4 = q^4\alpha$. The Green's function then becomes

$$G(r_1, r_2) = \frac{1}{(2\pi)^2\alpha}\int_{-\infty}^{\infty}dk_x\,e^{ik_xR}\underbrace{\int_{-\infty}^{\infty}\frac{dk_y}{(k_y^2 + k_x^2 - k_c^2)^2 - q^4 + i\delta}}_{I(k_x)} \tag{A.25}$$

To evaluate the integral $I(k_x)$, one must find the poles. $I(k_x)$ has six different sim-
ple   poles.

- There are six roots for $k_x^2 - k_c^2 > 0$;

$$k_{(y,1,2)} = \pm\mathrm{i}\sqrt{q^2 + k_x^2 - k_c^2} \pm \delta \qquad (A.26)$$

and

$$k_{(y,2,3,4,5)} = \begin{cases} \pm\sqrt{q^2 - k_x^2 + k_c^2} - \mathrm{i}\delta & \text{if} \quad k_x^2 < q^2 + k_c^2 \\ \mathrm{i}\sqrt{-q^2 + k_x^2 - k_c^2} \mp \delta & \text{if} \quad k_x^2 > q^2 + k_c^2 \end{cases} \qquad (A.27)$$
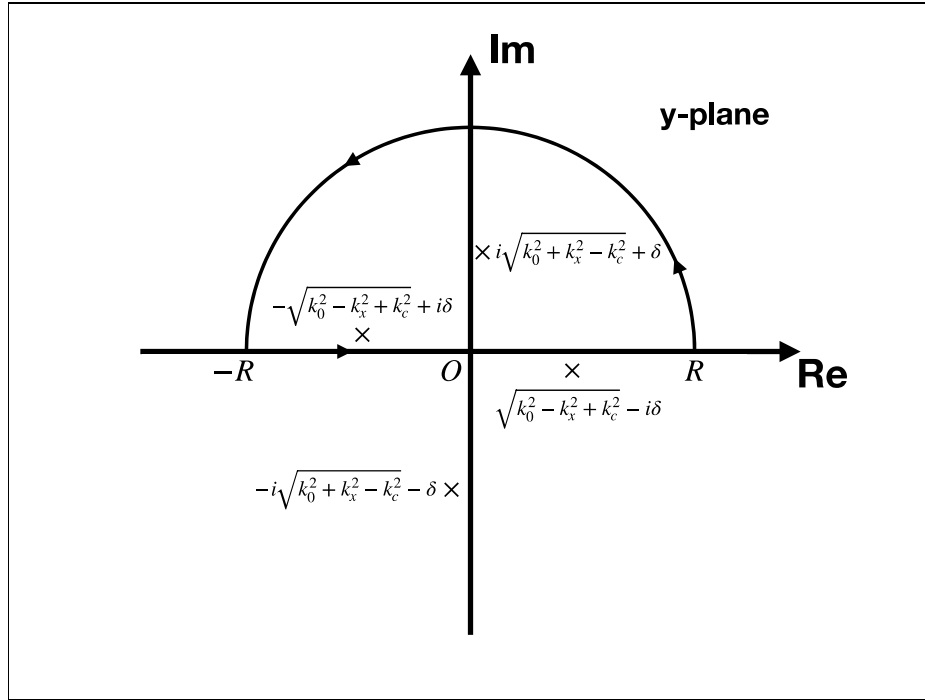

Figure A.3. The contour and the simple poles of the integral when $k_x^2 > k_c^2$.

- There are also six roots for $k_x^2 - k_c^2 < 0$;

$$k_{(y,1,2)} = \pm\sqrt{q^2 - k_x^2 + k_c^2} \qquad (A.28)$$

and

$$k_{(y,2,3,4,5)} = \begin{cases} \pm\mathrm{i}\sqrt{q^2 + k_x^2 - k_c^2} - \mathrm{i}\delta & \text{if} \quad k_x^2 < q^2 + k_c^2 \\ \pm\sqrt{-q^2 - k_x^2 + k_c^2} & \text{if} \quad k_x^2 > q^2 + k_c^2 \end{cases} \qquad (A.29)$$
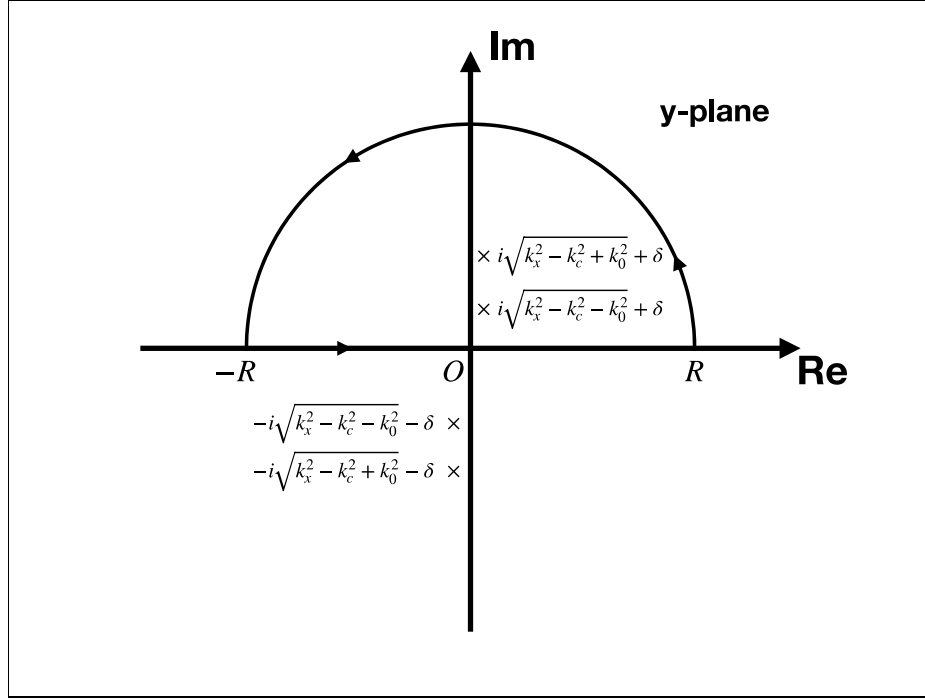
Figure A.4. The contour and the simple poles of the integral when $k_x^2 < k_c^2$.

For $q^2 > k_c^2 - k_x^2$, $(k_x^2 > k_c^2 - q^2)$

$$
\begin{aligned}
I(k_x) &= 2\pi\mathrm{i}\left[g\left(i\sqrt{q^2 + k_x^2}\right)\mathrm{Res}_{i\sqrt{q^2+k_x^2}}(f)\right. \tag{A.30}\\
&\quad + \left. g\left(-\sqrt{q^2 - k_x^2}\right)\mathrm{Res}_{-\sqrt{q^2-k_x^2}}(f)\right]\\[4pt]
I(k_x) &= 2\pi\mathrm{i}\left(\frac{\mathrm{i}}{4q^2\sqrt{q^2 + k_x^2}} - \frac{1}{4q^2\sqrt{q^2 - k_x^2}}\right)\\[4pt]
I(k_x) &= -\frac{\pi}{2q^2\sqrt{q^2 + k_x^2}} - \frac{\pi\mathrm{i}}{2q^2\sqrt{q^2 - k_x^2}}
\end{aligned}
$$

For $q^2 < k_c^2 - k_x^2$, $(kx^2 < k_c^2 - q^2)$

$$I(k_x) = 2\pi i \left[g\left(i\sqrt{q^2 + k_x^2}\right) \operatorname{Res}_{i\sqrt{q^2+k_x^2}}(f) \right. \tag{A.31}$$
$$\left. + \ g\left(i\sqrt{k_x^2 - q^2}\right) \operatorname{Res}_{i\sqrt{k_x^2-q^2}}(f) \right]$$

$$I(k_x) = 2\pi i \left(\frac{i}{4q^2\sqrt{q^2 + k_x^2}} - \frac{i}{4k_x^2\sqrt{k_x^2 - q^2}} \right)$$

$$I(k_x) = = \frac{\pi}{2q^2\sqrt{k_x^2 - q^2}} - \frac{\pi}{2q^2\sqrt{q^2 + k_x^2}}$$

Hence, the Green's function becomes

$$G(r_1, r_2) = \frac{1}{(2\pi)^2\alpha} \left(\int_{|k_x| > \sqrt{k_c^2 - q^2}} I(k_x)e^{ik_x R}\, dk_x \right. \tag{A.32}$$
$$\left. + \int_{|k_x| < \sqrt{k_c^2 - q^2}} I(k_x)e^{ik_x R}\, dk_x \right)$$

We can explicitly write as the following:

$$G(q, R) = \frac{1}{(2\pi)^2\alpha} \left[\int_{\sqrt{q^2+k_x^2}}^{\infty} - \left(\frac{\pi}{2q^2\sqrt{q^2 + k_x^2}} + \frac{\pi i}{2q^2\sqrt{q^2 - k_x^2}} \right) e^{ik_x R}\, dk_x \right. \tag{A.33}$$
$$+ \int_{-\infty}^{-\sqrt{q^2+k_x^2}} - \left(\frac{\pi}{2q^2\sqrt{q^2 + k_x^2}} + \frac{\pi i}{2q^2\sqrt{q^2 - k_x^2}} \right) e^{ik_x R}\, dk_x$$
$$\left. + \int_{-\sqrt{q^2+k_x^2}}^{\sqrt{q^2+k_x^2}} \left(\frac{\pi}{2q^2\underbrace{\sqrt{k_x^2 - q^2}}_{i\sqrt{q^2-k_x^2}}} - \frac{\pi}{2q^2\sqrt{q^2 + k_x^2}}\, dk_x \right) e^{ik_x R}\, dk_x \right]$$

The integrals can be rearranged in the form:

$$G(q, k_c, R) = -\frac{1}{8\pi\alpha q^2} \left[\int_{-\infty}^{\infty} \frac{e^{ik_x R}}{\sqrt{q^2 + k_x^2}}\, dk_x + i \int_{-\infty}^{\infty} \frac{e^{ik_x R}}{\sqrt{q^2 - k_x^2}}\, dk_x \right] \tag{A.34}$$

We should now consider two cases which are $q^2 > k_c^2$ and $q^2 < k_c^2$. After evaluating the integrals, we obtain the Green's function for the quartic dispersion,

for $q^2 > k_c^2$;

$$G(q, k_c, R) = -\frac{1}{8\pi\alpha q^2}\left[2K_0\left(\sqrt{q^2 - k_c^2}R\right) + i\pi H_0^{(1)}\left(\sqrt{q^2 + k_c^2}R\right)\right] \quad \text{(A.35)}$$

and for $q^2 < k_c^2$;

$$G(q, k_c, R) = \frac{i}{8\alpha q^2}\left[H_0^{(1)}\left(\sqrt{k_c^2 - q^2}\,R\right) + H_0^{(1)}\left(\sqrt{k_c^2 + q^2}\,R\right)\right] \quad \text{(A.36)}$$

where q is modified Bessel function and $H_0^{(1),(2)}$ are the Hankel functions of first and second kind.

We can now calculate the magnetic susceptibility using the Green's function for $q > k_c$.

$$\chi(R) = \int_{-\infty}^{E_f} \text{Im}\{G(q, R)^2\}\,\mathrm{d}E \quad \text{(A.37)}$$

If $E = -\alpha q^4$, then $\mathrm{d}E = -4\alpha q^3\,\mathrm{d}q$. Then, we have

$$\chi(R) = -\frac{1}{16\pi^2\alpha}\int_{-\infty}^{k_f} \frac{1}{q}\text{Im}\left\{\left[K_0\left(\sqrt{q^2 - k_c^2}R\right) + i\pi H_0^{(2)}\left(\sqrt{q^2 + k_c^2}R\right)\right]^2\right\}\,\mathrm{d}q$$

We know that $q(x)$ is real for $x > 0$. Furthermore, $J_0(x)$ and $N_0(x)$ are real for $x > 0$ therefore the Hankel function consists of real and pure imaginary parts because $H_0^{(1)}(x) = J_0(x) + iN_0(x)$. Using the lemma, we can write the integrand as follows

$$\chi(R) = \begin{cases} \frac{1}{8\pi^2\alpha}\int_{k_c}^{\infty}\frac{1}{q}\left[\left(K_0\left(\sqrt{q^2 - k_c^2}R\right) - \pi N_0\left(\sqrt{q^2 + k_c^2}R\right)\right)\right.\\ \qquad\qquad\qquad\qquad\left.\times\left(\pi J_0(\sqrt{q^2 + k_c^2}R)\right)\right]\,\mathrm{d}q \qquad\quad \text{for } E < \alpha k_c^4 \\ \\ \\ \frac{1}{8\alpha}\int_{k_f}^{k_c}\frac{1}{q}\left[\left(J_0(\sqrt{k_c^2 - q^2}R) + J_0(\sqrt{k_c^2 + q^2}R)\right)\right.\\ \times\left(N_0(\sqrt{k_c^2 + q^2}R) - N_0(\sqrt{k_c^2 - q^2}R)\right)\right]\,\mathrm{d}q \qquad\quad \text{for } E > \alpha k_c^4 \end{cases}$$